




Zn injection in Pressurized Water Reactors – laboratory tests, field experience and modelling

Authors

Iva Betova, Martin Bojinov, Petri Kinnunen, Timo Saario

Confidentiality

Public

Report's title Zn injection in Pressurized Water Reactors – laboratory tests, field experience and modelling	
Customer, contact person, address SAFIR 2014 research programme	Order reference
Project name Water chemistry and plant operating reliability	Project number/Short name 73786 / WAPA
Author(s) Iva Betova, Martin Bojinov, Petri Kinnunen, Timo Saario	Pages 60/
Keywords Zinc water chemistry, Pressurised Water Reactor, activity build up, corrosion mitigation, source term reduction	Report identification code VTT-R-05511-11
Summary <p>This report describes the use of zinc injection technology in Pressurized Water Reactor (PWR) plants worldwide. The review covers the range from basic information to current knowledge and understanding of operational behaviour. The basis of this report is the information available in the open literature, including proceedings of the recent International Conferences on Water Chemistry of Nuclear Reactor Systems. The influence of zinc injection in the primary circuit of PWRs on corrosion release, oxide growth on construction materials (stainless steels and nickel-based alloys), activity incorporation and source term reduction, fuel cladding corrosion, build-up and transformation of fuel crud, and Primary Water Stress Corrosion Cracking is described from the viewpoint of both laboratory testing and plant operational experience in France, USA, Germany and Japan. The perspectives to employ zinc water chemistry already at the stage of Hot Functional Testing, as well as for the use of zinc injection in WWERs are also presented and discussed. A substantial part of the present report is devoted to the recent experience in the modelling of the influence of zinc on corrosion and activity build-up in PWRs. Thermodynamic calculations of stability of different oxide phases and their solubility are critically reviewed. Solid-state chemical calculations of the defect structure of oxides on construction materials are also briefly reviewed. The kinetic modelling of the zinc adsorption on and incorporation into oxides on stainless steels and nickel-based alloys in simulated and in-pile PWR conditions is presented in detail and the significance of the derived kinetic parameters for the evaluation of the role of zinc in corrosion mitigation and activity build-up suppression is discussed. Finally, a formal linear system approach to the effect of zinc transients in PWRs is briefly outlined and an outlook of the current state-of-the art of our knowledge of zinc water chemistry and its future perspectives is given.</p>	
Confidentiality	Public
Espoo 8.9.2011 Signatures    Timo Saario Principal Scientist Leena Carpen Senior Scientist Pentti Kauppinen Technology Manager	
VTT's contact address P.O. Box 1000, FI-02044 VTT, Finland	
Distribution (customer and VTT) Customer 1 copy, VTT 1 copy	
<i>The use of the name of the Technical Research Centre of Finland (VTT) in advertising or publication in part of this report is only permissible with written authorisation from the Technical Research Centre of Finland.</i>	

Preface

This literature survey was compiled as part of the project “Water chemistry and plant operating reliability” within the SAFIR 2014 –research programme.

08.09.2011

Authors

Contents

1	Introduction	4
2	Goal	4
3	Description of the target	5
4	Influence of Zn injection on activity incorporation	6
4.1	Incorporation inventory in the RCS	6
4.2	Mechanism of activity incorporation	7
4.3	Influence of zinc on oxide growth, corrosion release and activity build-up	8
4.4	Experience with implementation of zinc chemistry	17
5	Influence of Zn on PWSCC	21
6	Influence of Zn on fuel	23
6.1	Performance of fuel cladding	23
6.2	Effect of Zn on fuel crud	25
7	Zn injection during HFT	27
8	Zn injection in WWERs	29
9	Modelling the effect of Zn injection	30
9.1	Thermodynamic modelling	30
9.2	Correlations between role of Zn and oxide structure	31
9.3	Kinetic modelling	33
9.4	System response to zinc transients	47
10	Conclusions and Outlook	50
10.1	Zinc impact on PWR primary chemistry	51
10.2	Zinc impact on fuel	52
10.3	Zinc impact on PWR dose rates	53
10.4	Outlook	53
11	Summary	54
	References	55

1 Introduction

In recent years, fuel performance and environmental issues take an important place in nuclear industry and consequently a number of objectives requested for an optimal water chemistry programme has been reviewed, such as reduction of radiation sources causing radiation exposures, integrity of structural materials and fuel cladding, and reduction of radioactive wastes and effluents.

Power-up rates, fuel burn-up and enrichment increases lead to high boiling duty conditions which enable crud deposition and consequently increase the probability for fuel cladding corrosion and/or Axial Offset Anomaly/Crud Induced Power Shift (AOA/CIPS) development. Hence, novel water chemistries have to be proposed and current water chemistry practices have to be revised in order to ensure optimal performance of the plant throughout its service life.

Zinc's ability to replace cobalt from oxides on primary circuit surfaces has provided the first motivation for implementing zinc addition in Boiling Water Reactors (BWRs) since the 1980s. The beneficial results regarding dose reductions have been demonstrated; therefore, this practice has been extended to Pressurized Water Reactors (PWRs) during the 1990s, not only for radiation fields' considerations, but also for reducing susceptibility to Primary Water Stress Corrosion Cracking (PWSCC).

First, zinc injection benefits relating to field radiation and SCC have been identified. After verification of the negligible effect of zinc injection on cladding integrity through laboratory and in-reactor testing, several field demonstrations have been performed progressively in more and more aggressive power reactors allowing concluding the absence of adverse effects on core performance linked to zinc injection. In parallel, the source term reduction and the modification of crud characteristics (morphology, structure and distribution) associated to the zinc injection have motivated to propose the zinc injection implementation, not only as radioprotection /materials tool, but also as way of preventing/mitigating the crud deposition in the core. Based on Nuclear Power Plant (NPP) feedback and laboratory tests, zinc injection is presumed to be able to answer to all the tasks requested, and it appears today as one of the key factors of primary coolant chemistry optimization for corrosion mitigation and source term reduction.

2 Goal

This report describes the use of zinc injection technology in Pressurized Water Reactor (PWR) plants worldwide. A review of the available laboratory work applicable to WWER plants is also included. The review covers the range from basic information to current knowledge and understanding of operational behaviour. The basis of this report is the information available in the open literature, including proceedings of the recent International Conferences on Water Chemistry of Nuclear Reactor Systems.

3 Description of the target

At the beginning of 1990's PWR vendors and utilities started to become interested in zinc injection because of the reported beneficial effect on dose reduction and corrosion inhibition from BWR experience. Therefore, comprehensive research work started mainly in two countries, US and Germany, to investigate the impact of zinc addition on material compatibility, fuel performance and operational conditions in PWR plants. In US the main interest was to mitigate PWSCC of Alloy 600 Mill Annealed (MA), a material that is used for SG tubing material and widely in many penetrations of the RCS. In collaboration with Westinghouse Owner's Group (WOG) and EPRI, Westinghouse initiated laboratory studies to examine the impact of zinc on PWSCC in the PWR primary water environment [1]. After completion of the investigation programs and performing plant specific qualification work, zinc injection was introduced in the US PWR plants. The Farley-2 plant was selected as the first candidate plant for zinc injection, as it had a sufficient number of cracked SG tubes to allow for a good statistical basis for monitoring of crack development. Zinc injection started in 1994 at Farley-2 plant, and followed by Diablo Canyon-1 and 2 in 1997-1998. In contrast to the US, PWSCC was not an issue for PWR plants in Germany due to use of Alloy 800NG as SG tubing material and avoidance of the use of Alloy 600MA in the RCS. The main interest for the German PWR utilities was radiation field reduction in their old PWR plants, which had rather high dose rates due to use of cobalt containing hard facing-materials (stellites) in the RPV internals. Siemens performed a research program in collaboration with VGB and German PWR utilities with the aim of studying the impact of zinc addition solely for dose reduction [2]. In Germany Biblis-B was the first PWR plant that introduced zinc injection in 1996, which was followed by Biblis-A and Obrigheim plants in the beginning of 1998. Due to convincing good field results from these lead plants that confirmed the beneficial effect of zinc chemistry, many PWR plants started to inject zinc in their reactor coolant. As of 2010, there are now almost 70 PWR plants that are injecting zinc (see Figure 1) [3].

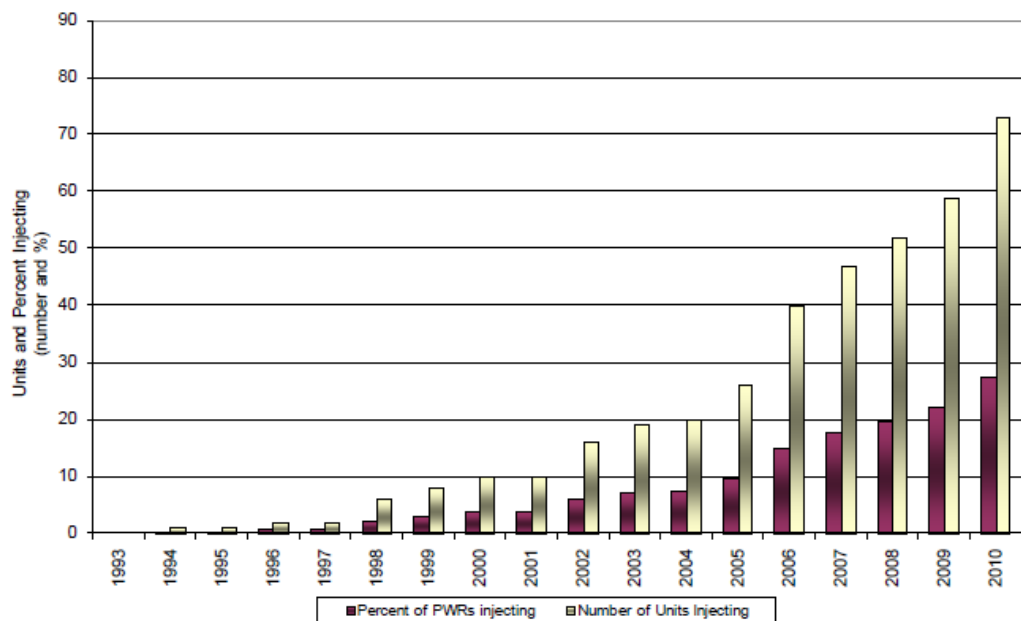


Figure 1 Number of PWR units injecting zinc worldwide [3].

4 Influence of Zn injection on activity incorporation

4.1 Incorporation inventory in the RCS

In a typical PWR, the wetted RCS surface area consists of approximately 25% fuel cladding (Zircaloy-4, Zirlo, or M5), 65% SG tubing (either a nickel-based alloy like Alloy 600MA, Alloy 600TT20, Alloy 690TT, or an iron-based alloy, Alloy 800NG) and about 10% stainless steel. The chemical composition of these materials is shown in Figure 2.

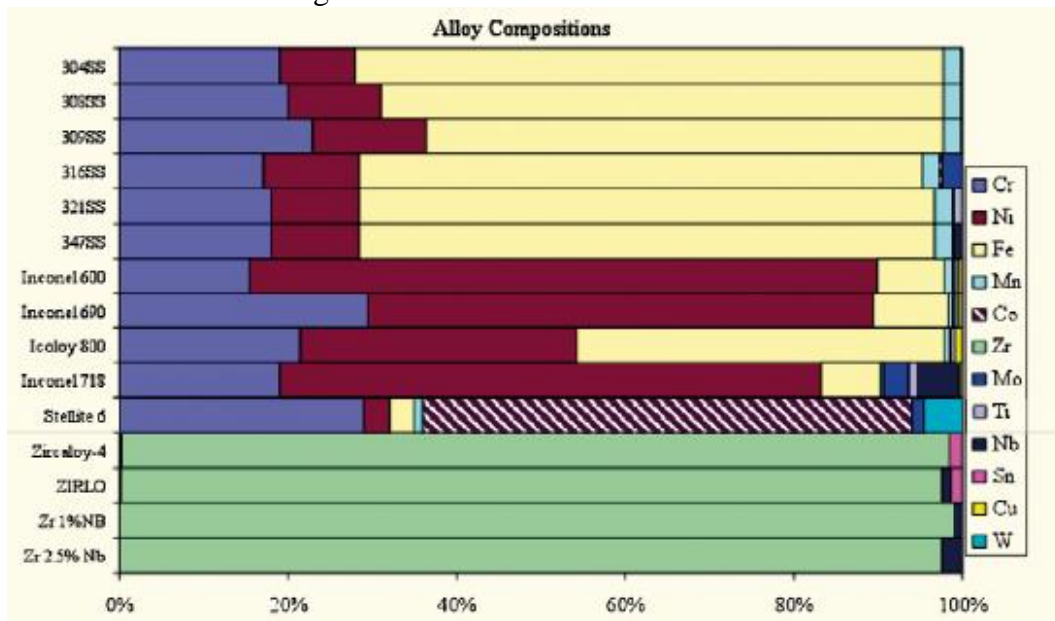


Figure 2 Nominal chemical composition of materials used in PWR plants.

At ambient temperatures all these construction materials have very low corrosion rates because of the formation of the passive oxide layers that protect them. With increasing temperature above 150 °C the general corrosion rate of these metals increases [4] because the passive oxide layers become thicker and more porous, albeit still protective. The composition and thickness of these protective layers depends on different factors, like the chemical composition of the base material, environmental conditions like the ECP, pH, coolant composition, and temperature of the medium to which they are exposed. The thickness of these protective oxide layers is in the range of several hundred nanometres. Oxide layers built under the PWR primary coolant operating conditions, i.e. reducing conditions at 300-330 °C, have duplex structure (Figure 3) [5,6]. They feature a chromium-rich inner layer and an iron and nickel-rich outer layer. The existence of duplex oxide layers is a result of different transport rates of the cationic substituents of the alloy or steel through the inner protective oxide layer. The inner oxide layer grows at its interface with the metal by anion mass transport although there is clearly iron and nickel cation transport in the reverse direction. The driving force for cation transport is the metal ion concentration difference between the metal surface and the coolant, as well as the field strength in the inner protective layer. Due to different diffusion coefficients of different metal ions their transport rates are also different. Iron and nickel exhibit much higher transport rates than chromium.

Therefore, the inner part of the protective oxide layer becomes chromium-rich, whereas the outer part is iron and nickel-rich.

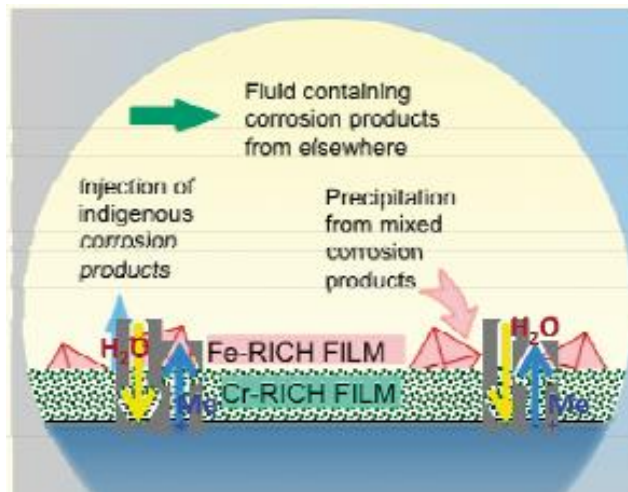


Figure 3 Structure of the protective oxide layers on stainless steel under PWR operating conditions

The iron and nickel-rich outer oxide layers are also more soluble in hydrogenated PWR primary water whereas chromium is for all practical purposes completely insoluble [7]. Therefore the growth of outer oxide layers is controlled by dissolution and precipitation of iron/nickel oxides. For example, if the outer layer is exposed to iron and nickel-free coolant in PWR primary water, only inner oxide layers and no outer layer are observed in the laboratory work due to dissolution of the outer layer [5]. On the other side, in iron-saturated coolant, large crystals of iron/nickel spinel oxide usually exist in this outer oxide layers that are produced from coolant by precipitation reactions. However, due to the higher solubility of iron/nickel oxides in hydrogenated PWR coolant, the oxide layers produced under reducing conditions of PWR reactor coolant are usually thinner than that produced under oxidizing BWR conditions.

4.2 Mechanism of activity incorporation

In the core region, a film consisting principally of zirconium dioxide (ZrO_2) forms on the zirconium alloy fuel assembly cladding, guide tubes and fuel grids. In addition to ZrO_2 , corrosion product deposits (nickel ferrites, metallic nickel and nickel oxides) are also found on fuel rods, which are precipitated from dissolved cations transported by coolant (see below).

On stainless steel and SG tubing, as mentioned above, duplex oxide layers with a nominal chemical composition of $Ni_xFe_{1-x}Cr_2O_4$ (nickel-iron chromite) for the inner layer and $Ni_xFe_{1-x}Fe_2O_4$ (nickel ferrites) for the outer layer are formed. If, a nickel base alloy is used for the SG tubing, the outer oxide layers on out-of-core surfaces can also contain metallic nickel. On fuel assembly rods, metallic nickel exists in the lower part of the core, whereas in the upper part, where boiling is expected, nickel exists usually as nickel oxide deposit. The solubility of these spinel oxide films is very low and they protect the materials very well.

Accordingly, the associated metal ion release is extremely low and their concentrations in the reactor coolant are in trace levels.

Even so, a certain amount of metal oxide does dissolve at the water-oxide interface and the solvated cations are transported by coolant flow to the core area, where they precipitate by boiling and/or due to their decreased solubility by increasing temperature (i.e. retrograde solubility). The deposited corrosion products are activated in the core area by the neutron flux and form ^{58}Co and ^{60}Co , according to the transmutation reactions $^{58}\text{Ni} (n,p) \rightarrow ^{58}\text{Co}$, and $^{59}\text{Co} (n,\gamma) \rightarrow ^{60}\text{Co}$. In turn, these nuclides are transported to and incorporated into chromium and iron spinel in the oxide layers on the surfaces of the primary circuit.

4.3 Influence of zinc on oxide growth, corrosion release and activity build-up

4.3.1 Zinc incorporation on RCS surfaces

According to theoretical hypotheses and experimental laboratory tests, the zinc injected into the primary coolant can have different destinations:

- It can be incorporated in the ex-core surfaces of primary system.
- It can be deposited on the fuel cladding
- It can be removed by CVCS system.

The amount of Zn incorporated into the primary circuit surfaces can be estimated as the difference between the Zn injected and the Zn removed. However, such a simplified calculation does not allow distinguishing between Zn incorporated in ex-core surfaces and that deposited on fuel assemblies. To describe more comprehensively the mass balance of Zn in the primary coolant taking into account the injection parameters, the characteristics of the unit and the cycle operation conditions, a model is proposed by Tigeras et al. [8]:

$$Zn_{(RCS-Incorporated)} = Zn_{(Injected)} - Zn_{(Removed-CVCS)}$$

Where each term can be evaluated by:

$$Zn_{(Removed-CVCS)} = [Zn]_{RCS} \frac{Q_{CVCS}}{M_{RCS}} t_{injection}$$

$$Zn_{(Injected)} = m_{Zn} * t_{injection}$$

$$Zn_{(Incorporated-RCS)} = \frac{[Zn]_{RCS}}{M_{RCS}} \left[\frac{Q_{SG}}{A_{tubingSG}} + \frac{Q_{SS}}{A_{RCS(SS)}} + \frac{Q_{fuel}}{A_{fuelclad}} \right] t_{injection}$$

With:

m_{Zn} : mass of zinc injected per day (g/day).

$t_{injection}$: temps of injection (day); A: Surfaces (m^2)

According to the authors [8], during the first phase of injection, until zinc reaches the detection limit ($\approx 1 \mu\text{g}/\text{kg}$), zinc removal is negligible and most of the zinc injected is incorporated into RCS surfaces. This process depends on daily injection quantity ($m(\text{Zn})$), area and material of each portion of the RCS (A_{SS} , A_{SG} , A_{fuel}) as

well as the incorporation rates into steam generators tubing films (Q_{SG}), stainless steels films (Q_{SS}) and fuel cladding crud ($Q_{fuel-clad}$).

$$\text{From } t=0 \text{ to } t=t_{\text{detection}}; Zn_{(RCS-Incorporated)} = Zn_{(Injected)}$$

$$t_{\text{detection}} = f(m_{Zn}, A_{SS}, Q_{SS}, A_{SG}, A_{fuel}, Q_{fuel}, P)$$

P =power; A_{SS} , A_{SG} , A_{fuel} =Surfaces

Where $Q=f(\text{thickness, composition of oxide films of Steam Generators (SG), stainless steels (SS) and crud (fuel)})$

Monitoring data with such calculated results on Zn are illustrated in Figure 4 for the first and second Zn injection cycles at two different plants [9].

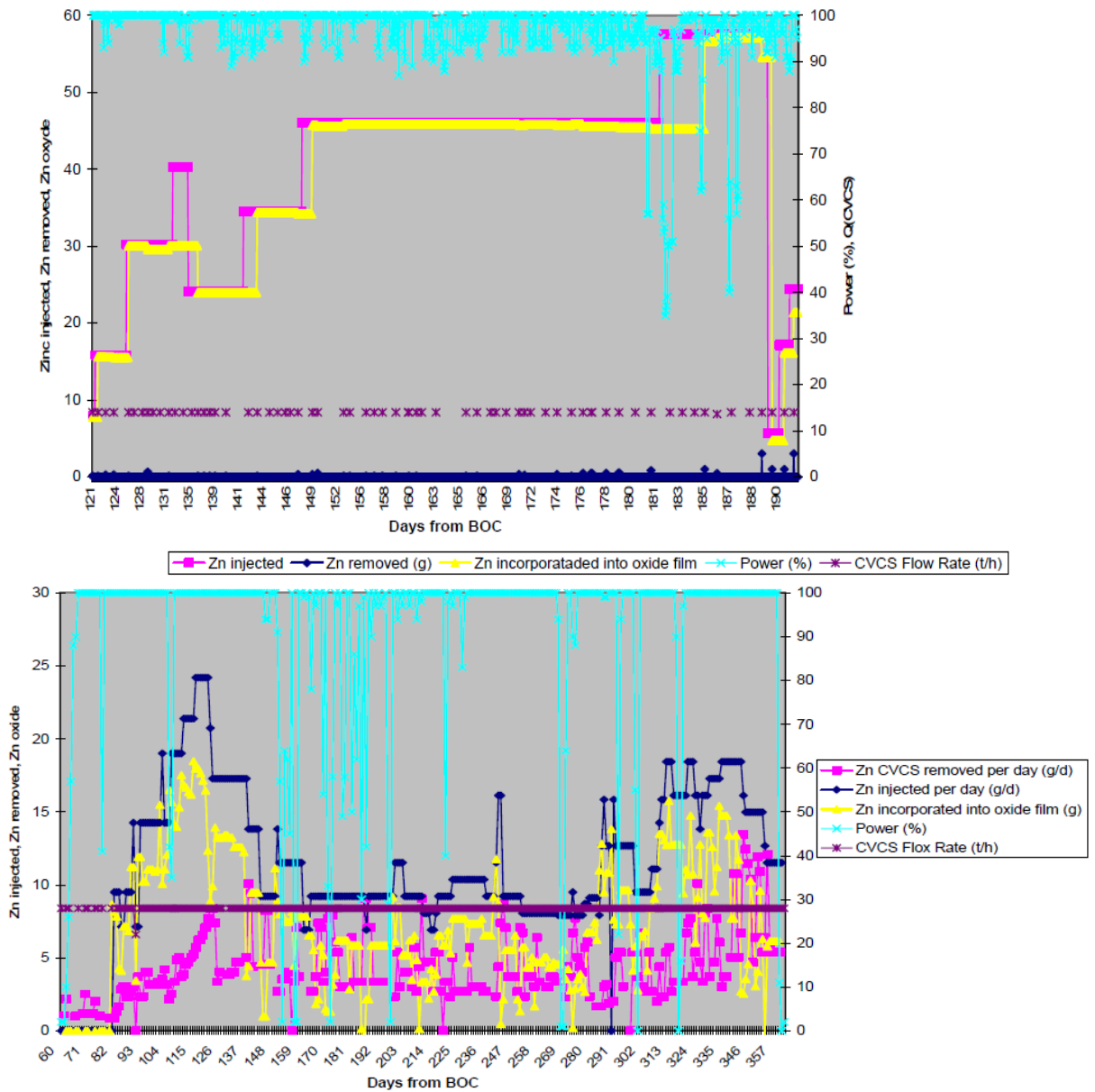


Figure 4 Zinc injected, removed and incorporated to the oxides during a first (above) and second (below) cycle of injection at two PWR plants.

4.3.2 Influence of zinc on oxide layers on out-of-core surfaces

Taking into account the RCS inventory and the contamination mechanism described above (sections 4.1 and 4.2), as well as the deposition process on fuel assemblies, a possible way to reduce the surface contamination and diminish the crud deposition is to find a non-radioactive element such as Zn capable of :

- Inhibiting the cobalt incorporation into the oxide layer of ex-core regions (mainly iron and nickel chromites FeCr_2O_4 , NiCr_2O_4 and nickel ferrite NiFe_2O_4) and/or
- Substituting the cobalt ions already incorporated in the oxide structures
- Diminish the corrosion release from primary circuit material.

If only the first process of inhibition is verified, it is predicted that dose rate reduction will be in correlation with the natural ^{58}Co and ^{60}Co activity decay (by 10 to 15% per year for ^{60}Co). Both paths of zinc influence are strongly believed to be related to the transformation of the protective oxide layers on construction materials in the presence of zinc.

Zn injection in PWR coolant can have a positive impact on corrosion phenomena by changing the chemical composition and structure of oxide films on austenitic stainless steels and nickel-based alloys [10]. However, the extent of the corrosion suppression effect of Zn that is due to modification of the protective properties of oxide films remains unquantified. Ziemniak et al. [11-13] claimed that corrosion films on 304 stainless steel (304 SS) in hydrogenated water with 30 ppb of injected Zn changed into thin oxide layers, which represent solvus phases in the $(\text{Zn}_m\text{Fe}_{1-m})(\text{Fe}_{1-n}\text{Cr}_n)_2\text{O}_4$ binary phase diagram. Recrystallization of the low outer zinc content ferrite solvus was proposed to impart additional resistance to corrosion. Beverskog [6] claimed, from thermodynamic calculation at 300 °C, that Zn injection did not lead to the formation of new solid phases (e.g. $\text{Zn}(\text{Fe}_x\text{Cr}_{1-x})_2\text{O}_4$) in pre-existing oxide films, that consisted of an outer NiFe_2O_4 and an inner FeCr_2O_4 oxide layer. This author presumed that ZnCr_2O_4 was only formed on new alloy surfaces exposed to the Zn-containing coolant. However, other thermodynamic calculations of Zn water chemistry in PWRs [14,15] showed that chromites (MCr_2O_4) have a higher stability than ferrites (MFe_2O_4) and ZnCr_2O_4 is the most stable phase within a wide potential -pH range and has the lowest solubility at 300 °C.

In a very recent paper [16], the oxide film on 304 SS exposed to simulated primary coolant with or without Zn was investigated by XPS, calculations of E-pH diagrams for the Zn-Fe-Cr-Ni-H₂O system and the solubility of spinels from 25–300 °C, as well as the crystallographic features of spinels were carried out to clarify the characteristics of the oxide film on 304 SS in the solutions with or without Zn injection. The following conclusions were drawn based on the results presented:

- Significant effects of Zn injection on the characteristics of the oxide film on 304 SS in the PWR environments were observed. In the Zn-free solution, a mixture of Fe_3O_4 and FeCr_2O_4 spinel oxides was most probably formed in the oxide film. Zn injection caused a drastic decrease of the thickness of that film (Figure 5). The oxide film formed in the presence of Zn was presumed to consist of ZnFe_2O_4 and ZnCr_2O_4 spinel oxides, and ZnCr_2O_4 would become dominant in the oxide film after long-term immersion.
- It was found that temperature has little effect on the E-pH regions of stability and solubility of different spinels in the studied PWR environments [16]. In

comparison with NiCr_2O_4 , FeCr_2O_4 , Fe_3O_4 , NiFe_2O_4 and ZnFe_2O_4 , ZnCr_2O_4 is the most stable within the widest E-pH range in the Zn-containing solution. The thermodynamically stable ZnCr_2O_4 with a low solubility under zinc water chemistry conditions indicates that the significant effect of Zn injection on the corrosion control of stainless steels in Zn-containing solution can be explained on the basis of an alteration of the phase composition of the inner layer of oxide.

- Based on the analysis of crystallography, temperature and ionic radius show no influence on the stability of the spinels. Zn^{2+} was demonstrated to prefer the tetrahedral sites in normal spinels. Considering the tetrahedral site stabilisation energies for cations in chromites and ferrites, ZnCr_2O_4 and ZnFe_2O_4 are proposed to be more stable in comparison with other possible spinels.

Other recent studies on AISI 316L(NG) stainless steel in simulated PWR coolant [17] have demonstrated that the effect of Zn injection on the thickness and composition of the oxides is very pronounced – the thickness of the oxide decreases ca. 6 times at open circuit and more than 2 times at 0.5 V vs. a reversible hydrogen electrode at 280 °C, the outer layer is practically absent (only a very thin layer containing boron was detected at the potential of 0.5 V) and the Cr content of the inner layer is significantly increased (more than twice, both at o.c. and at 0.5 V). Zn is incorporated in the oxide at both potentials in significant amounts (a normalised content of several %), its concentration being somewhat larger in the film formed at open circuit. It can be concluded that the injection of 1 ppm Zn to the simulated PWR water causes a dramatic restructuring of the oxide formed on stainless steel for 24 h in Zn-free solution. Part of this effect could be attributed to the decrease of pH due to the hydrolysis reactions of Zn. Thus further investigations have been performed in a buffered high-pH PWR coolant [17].

In the presence of tetraborate, the thicknesses of the films in both Zn-free and Zn-containing electrolytes are more than 2 times larger than those formed in solutions that did not contain tetraborate. This effect could be related to the decrease of the solubility of Fe with increasing pH. Such an explanation is corroborated by the fact that outer layers (i.e. layers that are formed by a dissolution-precipitation mechanism) are observed in both Zn-free and Zn-containing electrolytes and their thickness is larger than that of the inner layer. The changes of the in-depth composition of the oxide caused by Zn injection are not as drastic as in the plain PWR water, even if the incorporation of Zn especially in the outer layer is really significant (above 20% of normalised content). This probably means that the outer layer formed by restructuring of the oxide following Zn injection is in fact a mixed Fe-Zn oxide containing small amounts of Ni and Cr. On the other hand, the amount of Zn incorporated in the inner layer stays close to that in the unbuffered PWR water. A notable effect of Zn injection is that the Ni content of the inner layer formed as a result seems to be larger than that of Cr, which is opposite to the inner layer formed in the absence of Zn. Thus Zn incorporation seems to play an important role in the restructuring of the inner layer also in tetraborate-containing PWR water [17].

Concerning oxide films formed on nickel-based alloys such as 600 and 690, Ziemniak et al. [18,19] claimed that the two-layer corrosion oxide with an inner layer of $\text{M}(\text{Fe}_{1-x}\text{Cr}_x)_2\text{O}_4$, on nickel-based alloys exposed in the simulated primary coolants with Zn injection transformed into a chromite-rich spinel oxide phase, $(\text{Zn}_{0.55}\text{Ni}_{0.3}\text{Fe}_{0.15})(\text{Fe}_{0.25}\text{Cr}_{0.75})_2\text{O}_4$, and recrystallized metallic nickel. The

replacement of Ni^{2+} and/or Fe^{2+} by Zn^{2+} also resulted in outer smaller sized ferrite-based crystals that retarded ingress of water towards the inner layer. Kawamura et al. [20] reported that the thick oxide film consisting of $\text{Fe}_x\text{Ni}_{1-x}\text{Fe}_2\text{O}_4$ and $\text{Fe}_x\text{Ni}_{1-x}\text{Cr}_2\text{O}_4$ on Alloy 600 without Zn injection transformed into a thinner and more stable $\text{Zn}_y + z\text{Fe}_{x-y}\text{Ni}_{1-x-z}\text{Cr}_2\text{O}_4$ spinel in simulated PWR primary water with Zn injection. The outer $\text{Fe}_x\text{Ni}_{1-x}\text{Fe}_2\text{O}_4$ layer might have become thinner or disappeared, leaving the inner chromite responsible for the reduction in primary water general and localised corrosion modes.

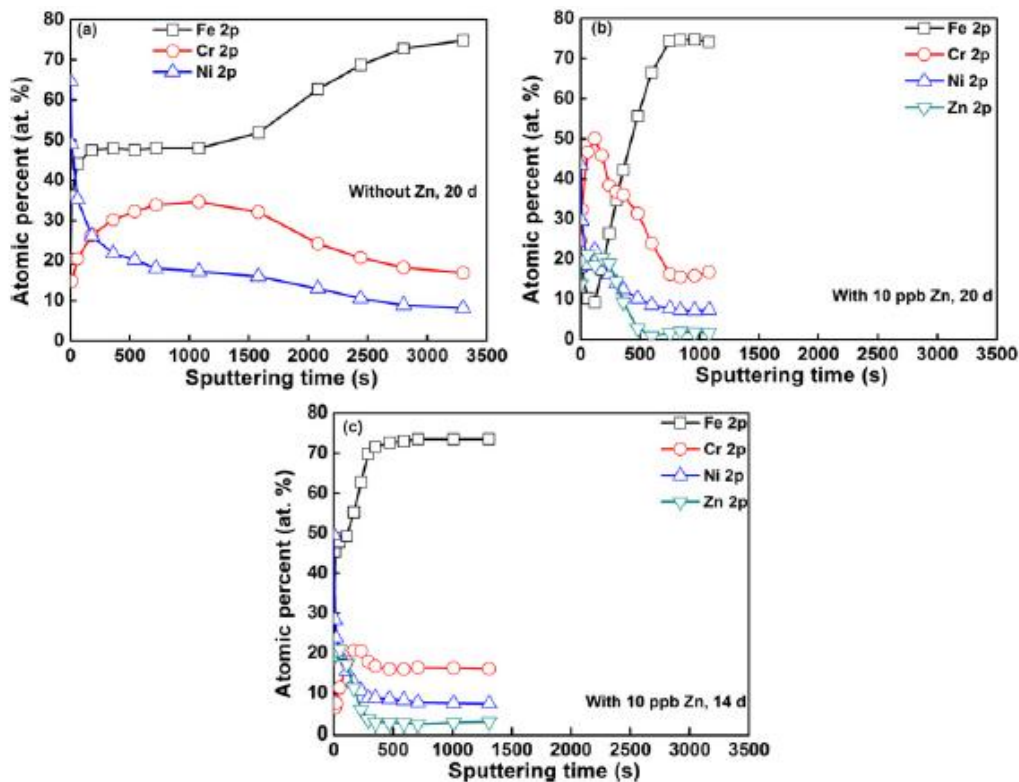


Figure 5 XPS depth profiles of the oxide films on 304 SS at 300 °C: (a) Zn-free solution after 20 d exposure, (b) Zn-containing solution after 20 d exposure and (c) Zn-containing solution after 14 d exposure [16].

Very recently, the effect of Zn injection on Alloy 690 was investigated in deaerated borated and lithiated water at 300 °C using voltammetric and electrochemical impedance spectroscopic measurements [21]. The chemical compositions of the oxide films formed were examined using XPS (Figure 6). The following conclusions were drawn from the data:

- The chemical compositions and the structures of oxide films formed on Alloy 690 changed with Zn injection. The oxide films consisted of Zn–Cr/Zn–Fe spinel oxides. The content of Ni in oxide films decreased rapidly and the oxide film became thin. With increasing Zn concentration, the resistance of the oxide film increased rapidly and the passive current density decreased.
- Due to the low free energy of formation of spinel oxides, Zn^{2+} displaced Ni^{2+} and/or Fe^{2+} in the tetrahedral sites in the crystal lattice. The incorporation of Zn into the spinel oxides would slow down transport of solid state point defects in the oxides by decreasing their concentration. An oxide film composed of $\text{Zn}(\text{Fe}_x\text{Cr}_{1-x})_2\text{O}_4$ was formed on Alloy 690 with Zn injection.
- It is suggested that the change of oxide film characteristics induced by Zn injection cause an improvement in the corrosion resistance of Alloy 690.

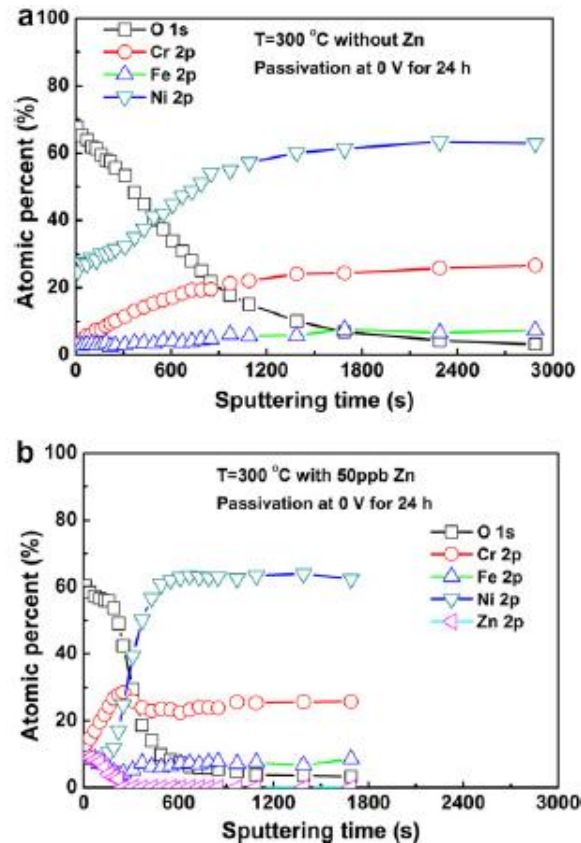


Figure 6 Composition depth profiles obtained from XPS analysis for the oxide film on Alloy 690 passivated for 24 h at 300 °C: (a) Zn-free solution, (b) 50 ppb Zn-containing solution.

These recent studies and related information on the effect of zinc water chemistry on structural materials have been concisely reviewed [22]. For more details on the state-of-the-art of modelling the effects of Zn in PWRs, the reader is referred to the Modelling Section 9 below.

4.3.3 Impact of zinc on corrosion release rates

It has been inferred from laboratory data that zinc uptake into fresh surface oxide formation resulted in a reduction of the corrosion rate and release rates of stainless steel, Alloy 600, and Alloy 690 materials as shown in Table 1 [25,26].

Numerous tests have been conducted in order to determine the zinc effect on alloys corrosion. The zinc incorporation into the oxide layer increases the stability and ductility of the oxide protective film and accelerates the passivation process [8]. The positive effect of zinc on corrosion and corrosion release has been demonstrated by the following observations:

- Decrease of corrosion rates not only for the alloys 600MA, 600TT and 690 T, but also for materials such as steels and stellites (Table 1) [25].
- Decrease of Ni release rates. The kinetics of the Ni release of 690 SG tube were measured in the PETER Loop [26]. The addition of 5 µg/kg Zn in the primary environment (Li=2 ppm, B=1200 ppm, H₂= 25 cm³/kg, T=325°C) significantly reduced the Ni release rates (Figure 7, above). The effect of Zn addition on Fe release rates was quite insignificant during these tests, except for an initial increase of soluble Fe (Figure 7, below) [27,28].

Table 1 Effect of Zinc on Approximate Corrosion and Corrosion Release Rates at 3.5 Months (mg/dm²/month)

Material	Corrosion		Corrosion Release	
	With Zinc	Without Zinc	With Zinc	Without Zinc
304 SS	1.1	3.5	0.1	1.3
316 SS	1.3	3.5	0.1	1.4
600 MA	1.5	2.6	0.3	0.8
600 TT	0.5	2.1	0.2	0.9
690 TT	0.2	1.3	0.1	0.6
X-750	0.6	2.6	0.2	1.2
Stellite	0.4	14.7	0.1	12.0

By reducing corrosion rates and corrosion product release rates, corrosion product generation and transport to the core is reduced. Thus Zn injection serves as a key component to the plant source term mitigation strategy.

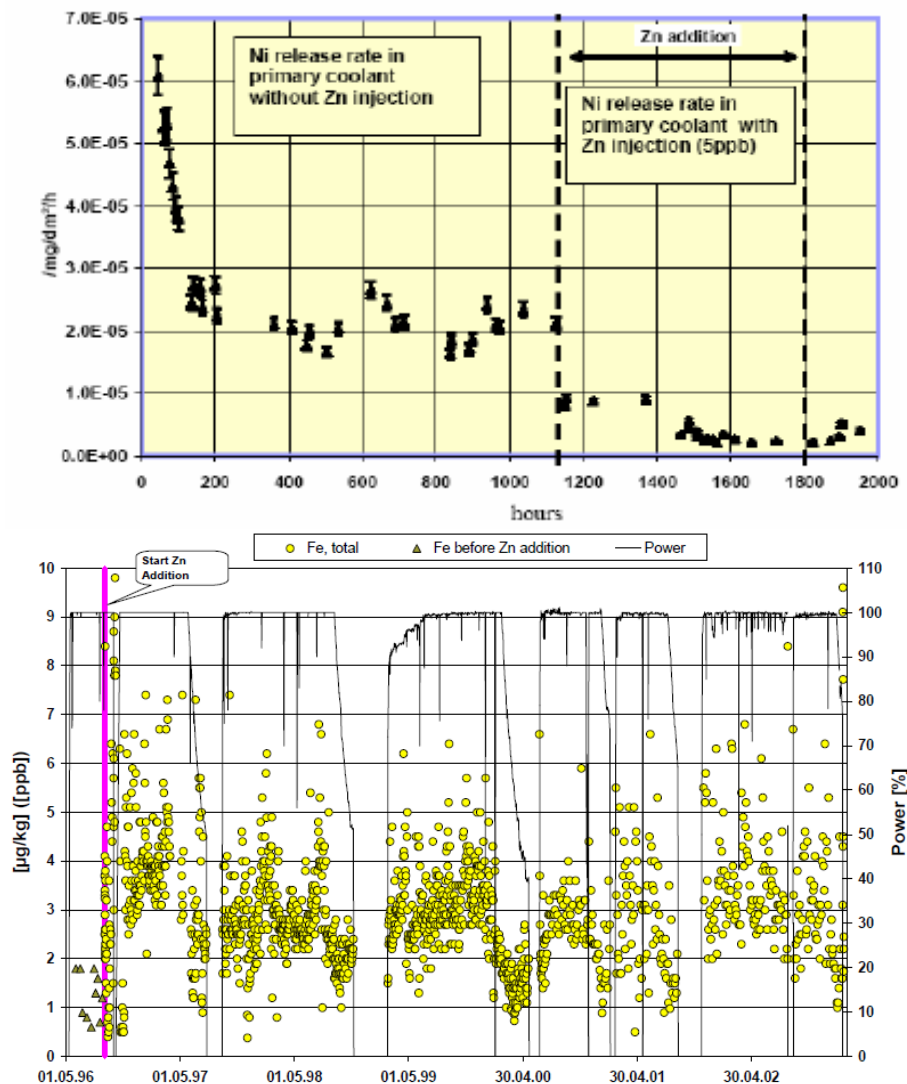


Figure 7 Impact of Zn injection on Ni (above) and Fe (below) release rates.

4.3.4 Radiation fields

The studies relative to the behaviour of zinc in primary coolant show that zinc can affect two main parameters: pH and cobalt–nickel activity [6,10,24]. Zinc hydrolysis in primary coolant may have an impact on e.g. surface pH, which can be lowered inducing an increase in oxide solubility and contributing to raise the corrosion product activity in primary coolant. Moreover, the radiocobalt activity levels in the coolant were expected to increase due to the substitution mechanism between the zinc and nickel/cobalt ions. As an example, the radiocobalt activity in the coolant is plotted with the zinc concentration at Bugey 4 during the first cycle of zinc injection (Figure 8).

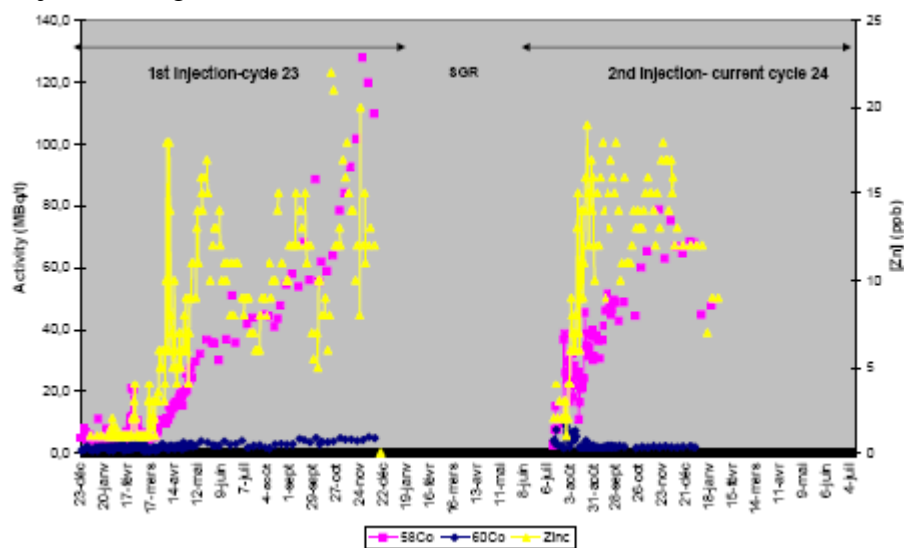


Figure 8 Correlation between soluble Zn concentration and radiocobalt activity evolution in RCS at Bugey 4 [24].

The surface activity deposit reduction, thanks to the Co replacement and/or suppression of Co incorporation on RCS oxide surfaces [10] is illustrated in Figure 9. The initial concern attributed to activity increase in the primary coolant is not confirmed by NPP operating experience. This fact can be explained by the progressive incorporation of Zn into the inner layer of oxide rich in chromites and by the optimal pH control permitting to limit the transfer and the activation of Co replaced from oxide layers.

The dose rate impact of zinc injection is documented in the EPRI *PWR Primary Water Chemistry Zinc Application Guidelines* and shows that with increasing zinc exposure (ppb-months), plant dose rates will be lower [24,25]. The trends are divided based on Alloy 600, 690 and 800 plants as well as the use of depleted and natural zinc. A simplified scheme of the role of zinc in the reduction of radiation fields by suppressing the corrosion release and modifying the oxide films on primary circuit surfaces is presented in Figure 11 [29].

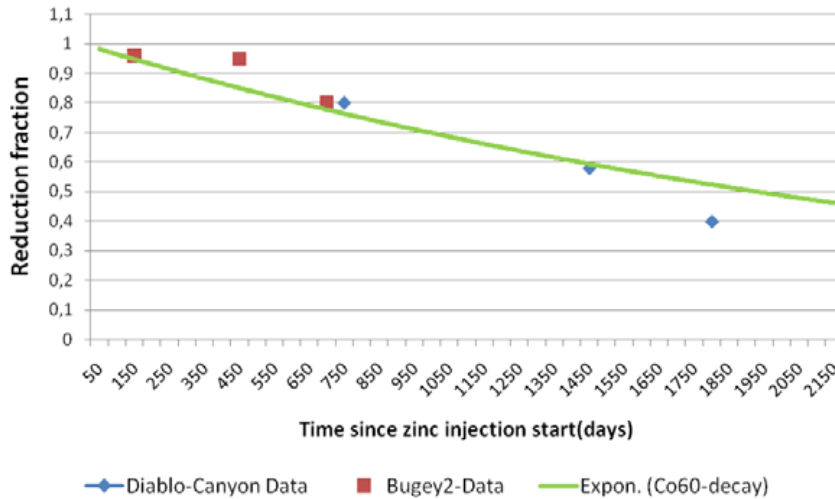


Figure 9 Confirmation of cobalt inhibition by zinc injection: ^{60}Co surface activity reduction.

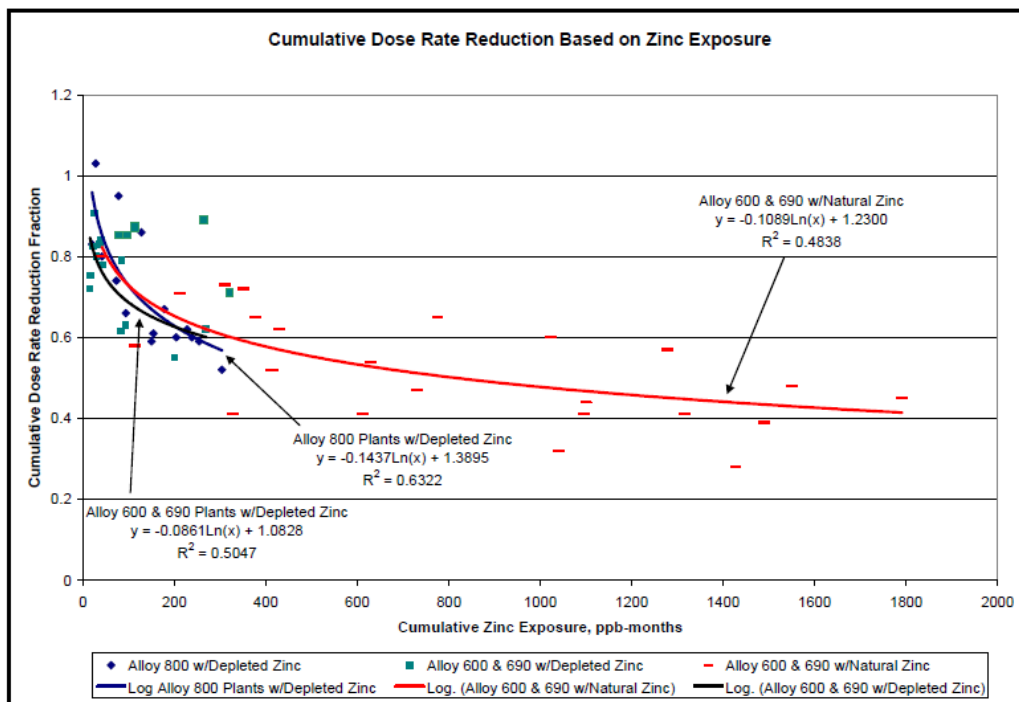


Figure 10 Dose Impact from Zinc Injection

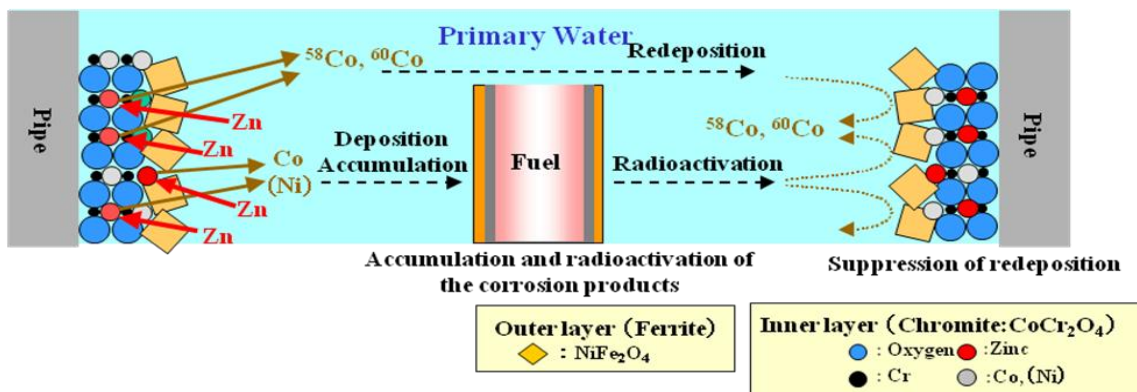


Figure 11 Presumptive mechanism of corrosion product behaviour with zinc in the primary coolant (from Ref.29).

4.4 Experience with implementation of zinc chemistry

4.4.1 Zinc compounds and their solubility

The main concern for the zinc injection during the first years of operation of the plants was to be sure all the time that fuel integrity and performance is not affected by possible zinc precipitation on the fuel rod surfaces and/or in the fuel deposits in particular, in the region of subcooled nucleate boiling (SNB). Therefore, zinc solubility behaviour under PWR coolant conditions with varying temperatures, pH values was one of the important subjects for the PWR industry investigations. The previous data regarding the solubility of the zinc compound were established by temperature extrapolations of ZnO solubility data, which were known for temperatures at ≤ 200 °C, to 300 °C. These extrapolations resulted in a conservative solubility limit of ≤ 40 $\mu\text{g}/\text{kg}$. Another prediction of 80 to 110 $\mu\text{g}/\text{kg}$ for zinc oxide solubility was also used by PWR industry, which was based on some conventional, limited data (in aqueous phosphate solutions) gained from previous studies [30]. Finally, at the beginning of 2000s, the Oak Ridge national Laboratories (ORNL) had performed experimental investigations to measure the solubility of zinc compounds under PWR coolant conditions at different temperatures and pH values. The results of their work can be summarized as follows [31- 33]:

- The solubility of zinc at the pH values of PWR operating conditions is between 100 and 200 $\mu\text{g}/\text{kg}$, depending on temperature between 150 and 350 °C (see Figure 12 for 200 and 300 °C as example).
- In the steam phase that is relevant for boiling on fuel rod surfaces, the solubility is about 1 $\mu\text{g}/\text{kg}$ as expected (see Figure 13).

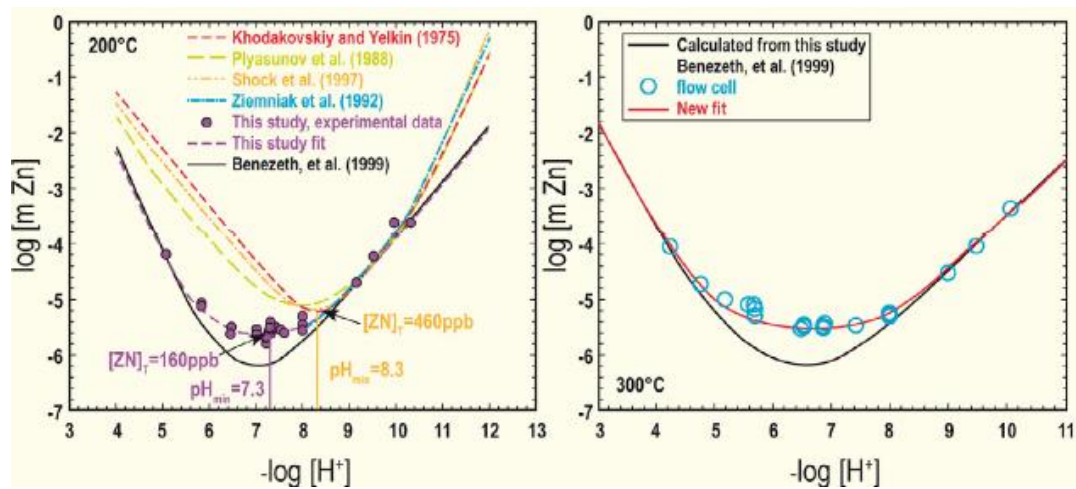


Figure 12 Solubility of zinc at 200 and 300 °C as a function of $\text{pH}_T (= -\log [H^+])$ values [33].

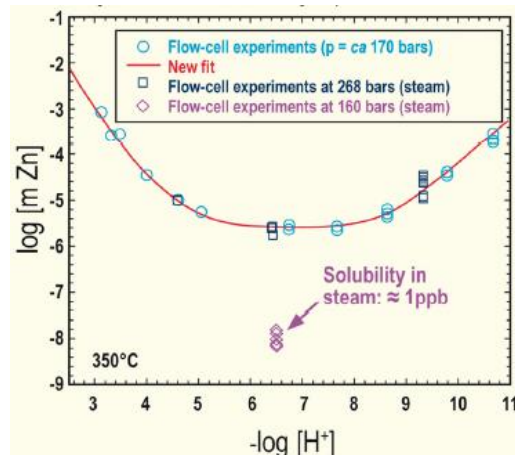


Figure 13 Solubility of zinc at 350 °C as a function of pH_T values [33].

Wesolowski et al. [33] have also calculated from the solubility constants, the distribution of aqueous zinc species as a function of pH and temperature as shown in Figure 14. It follows that in the near neutral pH to mildly basic region relevant for PWR coolant conditions, the dominating species are $Zn(OH)^+$ and $Zn(OH)_2$ and not the Zn^{2+} . As temperature increases, $Zn(OH)_2$ and $Zn(OH)_3^-$ become predominant.

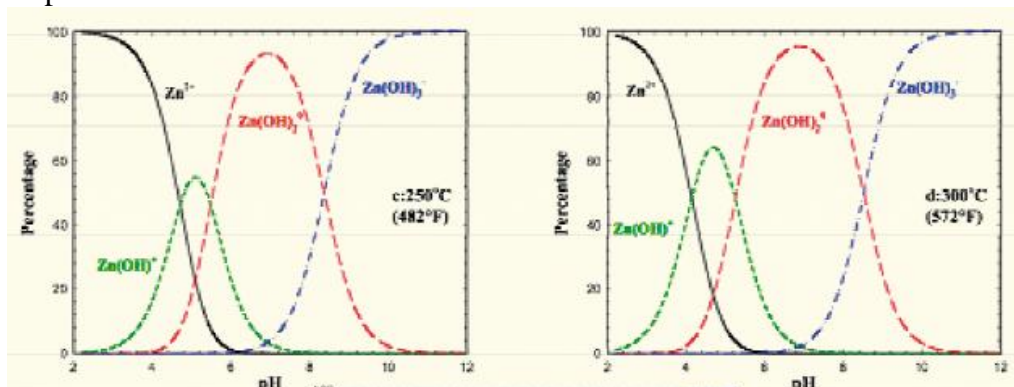


Figure 14 Distribution of aqueous zinc species as a function of pH at different temperatures [33].

4.4.2 Zinc injection concept

Zinc injection consists of a continuous addition of zinc in the primary coolant. A system of injection and a suitable zinc form have to be selected in order to assure the absence of impact on the installation and to limit the possible changes on site organization. This paragraph intends to provide some indications that can be useful for the zinc injection implementation in future units.

The natural zinc addition at Diablo Canyon 1&2, Farley1&2 and Beaver Valley has shown a smaller dose radiation benefit during the first cycles of injection and ^{65}Zn activity increase in primary coolant. All the other PWRs began the injection using depleted zinc from the first cycle in spite of the supplementary cost associated with the depletion process. Nowadays, all the PWR use depleted zinc with <1% wt. ^{64}Zn . No negative dose impacts have been reported and the ^{65}Zn activity has always remained at the same levels than before the beginning of the zinc injection. The selection of depleted zinc vs. natural zinc has been justified by the ^{65}Zn limitation

in the oxide layers of primary circuit surfaces, in order to optimize the dose rate, effluents and waste benefits.

With the objective of making the dissolution of zinc easy and avoiding capillary obstructions, a weak acid was researched in order to increase the reagent solubility. The possible injection of zinc borate ($x\text{ZnO}\cdot y\text{B}_2\text{O}_3\cdot z\text{H}_2\text{O}$), zinc formate ($\text{Zn}(\text{HCOO})_2\cdot 2\text{H}_2\text{O}$) and zinc acetate ($\text{Zn}(\text{CH}_3\text{COO})_2\cdot 2\text{H}_2\text{O}$) was initially evaluated. Several tests confirmed the inadequacy of zinc borate because of its low solubility. On the other hand, the zinc injection into RCS requires a low level of impurities. The fabrication process of zinc formate at high purity is much more expensive than that of zinc acetate, which is nowadays produced with a reasonable cost for industrial needs.

Hence, zinc acetate has been selected for its high solubility (430 g l^{-1} at 25°C) and high purity. Moreover, the introduction of every product e.g. in EdF reactors needs to respect a homologation process, permitting to assure the security and the safety of both staff and installations. Zinc acetate was granted the PMUC (Products and Materials used in Power Plants) homologation and this product is considered by the international regulation as a “nonhazardous substance” due to its nature (nonexplosive, inflammable and noncombustible). Therefore, zinc acetate manipulation by the chemistry staff can be done using the habitual standards of safety.

4.4.3 Zinc injection system

The zinc injection equipment has been selected considering:

- Injection location - the injection point is usually placed in the sampling lines with return to the VCT and the zinc injection system is in the room used by the chemistry staff for sampling (Figure 15). These decisions aim to assure a correct and regular maintenance by the personnel in charge of the zinc injection application.
- Injection equipment - simplicity has been privileged in order to avoid possible interruptions of injection during the cycles due to mechanical and/or electronic causes linked to possible complexities of the devices. The selected system of injection includes a tank, a volumetric pump and the appropriated accessories of safety (valves, level measurements).
- Measurement and control equipment - the zinc injection requires the monitoring of zinc, nickel and silica. The necessity to verify the limits imposed by the chemical specifications has led to develop specific procedures for each element and technique (AAS and ICP).

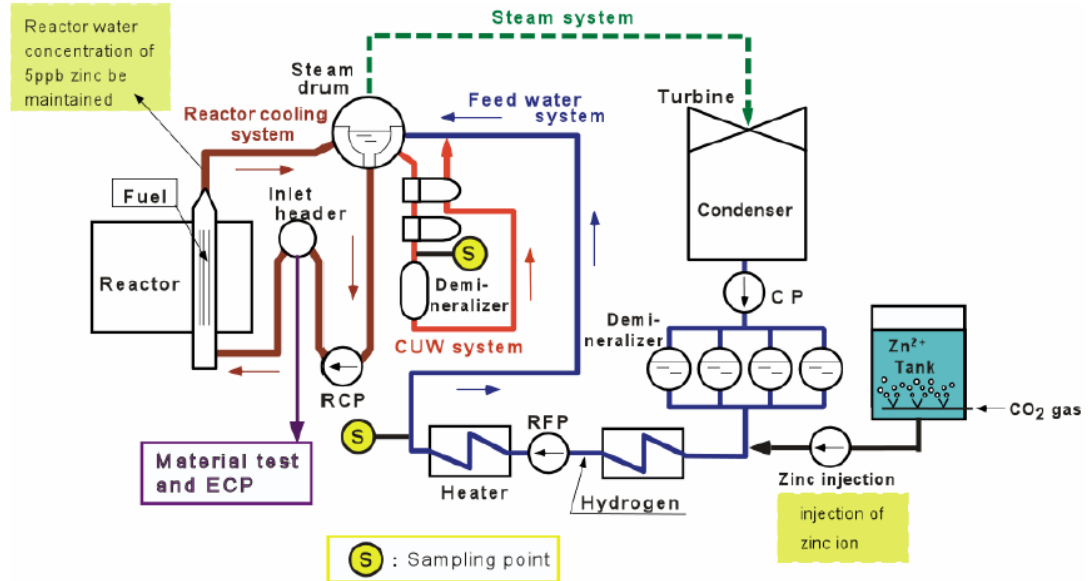


Figure 15 Outline of a typical zinc injection system.

4.4.4 Chemical specifications of zinc injection

4.4.4.1 Nickel limits

The crud analysis from PWR shows that nickel is present in both metallic form and nickel oxide precipitate in the upper regions of fuel assembly with high boiling. In order to minimize this potential deposition, the nickel concentration in the coolant is limited and its evolution is regularly monitored according to the chemical specifications. The maximum value admitted by fuel suppliers for beginning the zinc injection is 6 ppb. This limit has been justified by the international feedback. In fact, nickel concentrations higher than 6 ppb have been measured during some cycles affected by AOA. On the contrary, the average nickel concentration at stable power in units not affected by AOA varies from 0.4 and 4 ppb [25]. In a conservative way, several utilities have introduced a more restrictive limit of 3 ppb for the high duty plants and for the cycles with high zinc concentrations (Figure 16).

4.4.4.2 Iron concentration

In the short term, the iron concentration increased in some German plants following the zinc injection beginning due to the presence of Alloy 800 (iron base alloy) steam generator tubing. The iron concentration in primary coolant has not been modified in units with 600 or 690 alloy (nickel base alloy). Therefore, no limit is required for these units and the iron monitoring is recommended but not mandatory by fuel vendors.

4.4.4.3 Silica limits

Zinc silicates have never been found in PWR fuel deposits, but they were found in some BWR deposits. Thermodynamic calculations show that zinc silicate is less likely to precipitate than zinc oxide under typical reactor coolant conditions. In a conservative way, the initial silica upper limit was fixed at 1 ppm by the fuel vendors. Research carried out by Westinghouse under EPRI funding [34] have permitted to establish the boundary operational conditions under which PWRs can

add zinc without fear of encountering fuel-related problems. The results show that the zinc silicates are deposited at high concentrations of silica ($\text{SiO}_2 > 10\text{ppm}$) and in presence of thick crud. These conclusions are corroborated by the positive feedback of some units injecting zinc with high silica levels ($\text{SiO}_2 > 2\text{ppm}$). Taking into account the above criteria, the most restrictive silica value for high duty plants and/or cycles with high zinc concentrations is set to 1 ppm (Figure 16).

4.4.4.4 Impurity limits

The Ca, Al and Mg concentration is limited to 0.05 mg/kg for NPP with and without zinc injection.

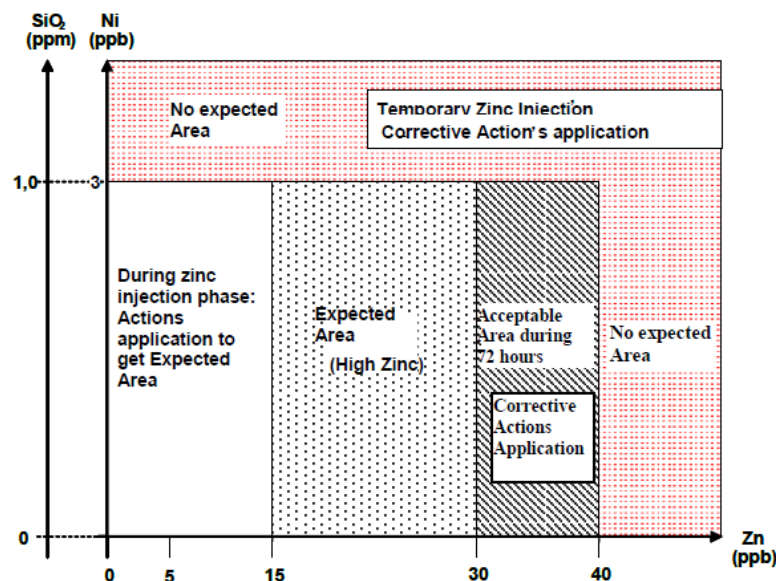


Figure 16 Boundary conditions of zinc injection application for high duty plants and/or high zinc concentration.

5 Influence of Zn on PWSCC

Zinc addition has been demonstrated to have a strong mitigative effect on the initiation of PWSCC in Alloy 600 [25]. This conclusion is based on strong evidence from assessments of in-service steam generator tube cracking [36,37]. Additional support is provided by extensive laboratory testing and mechanistic investigations [20,25,38-45]. Test results for nickel alloys are summarized in Figure 17. In Ref. 20, it was assumed that PWSCC initiation consisted of the following four processes: formation of double-layered oxide film; selective dissolution or destruction of metallurgically disordered regions, such as grain boundaries where applied stress is concentrated and chromium content is lower; appearance of fresh alloy surface; and initiation of a PWSCC crack. When ≥ 10 ppb Zn was added to the simulated PWR primary water, however, PWSCC susceptibility of Alloy 600MA decreased, even when oxide films were formed via preoxidation in zinc-free simulated PWR water. This was hypothesized to be a result of suppression of hydrogen reduction on the surface, diminishing or thinning of the outer layer, and formation of a chromium-enriched protective film containing zinc on Alloy 600MA. Further studies focused on crack growth rather than initiation have shown, however, that the Zn effect on crack growth becomes questionable at high enough stress intensity factors [42,44]. According to the authors, fast-growing cracks require

that Zn permeate to the crack tip while also saturating / equilibrating into the new oxide as the crack advances, and thus impact of Zn on such cracks might be limited.

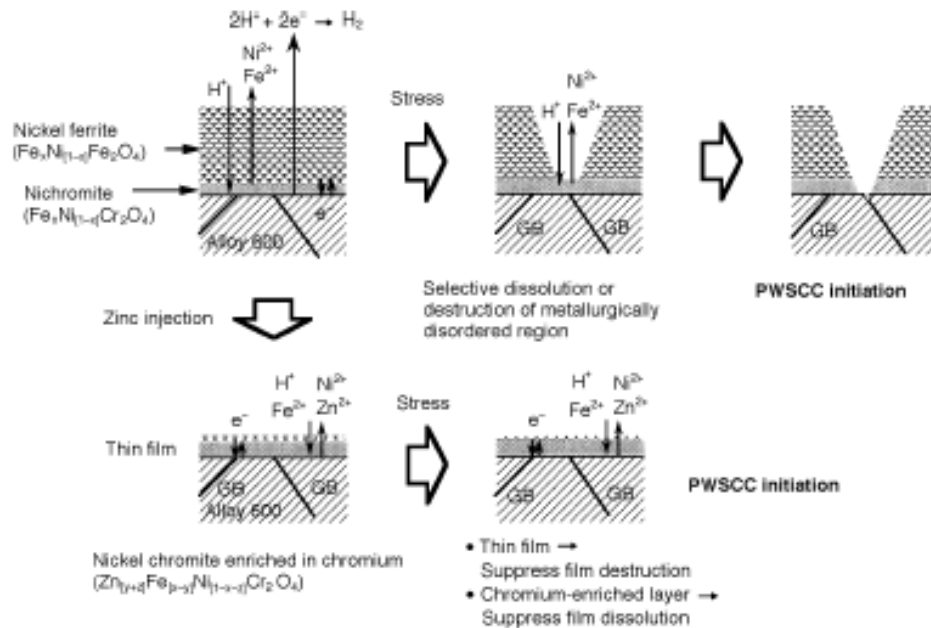


Figure 17 Oxide film structure changes and PWSCC suppression mechanism of Alloy 600MA by zinc injection [20,41].

Concerning in-plant data, Figure 18 illustrates the benefit of zinc addition at a plant that has been injecting zinc at a nominal RCS concentration of 5 ppb. The data are based upon the cumulative number of PWSCC indications at explosively expanded (WEXTX) regions in the tube sheet and on carefully screened non-destructive evaluation (NDE) data, and are plotted as a Weibull analysis. (Note that this plant shot-peened at between 5 and 6 effective full power years (EFPY)). The rate of degradation is reflected in the slope of the Weibull plot, with a smaller slope corresponding to a decreased rate of SG tube degradation. As observed from Figure 18, the rate of PWSCC indications has decreased significantly since zinc injection. At about 14 EFPY the percentage of tubes affected was almost 1% (and corresponded to the time when zinc injection was initially begun). Based on an evaluation completed in 2005 [36], zinc injection resulted in an improvement factor of about 2 (i.e., it would take twice as long to reach 10% tubes affected based on the then current post-zinc Weibull slope as compared to the pre-zinc Weibull slope). According to another evaluation completed in 2008 [37], zinc injection has resulted in an improvement factor of about 10. Thus, zinc injection continues to significantly reduce the rate of new PWSCC indications over time.

With regard to crack growth rates in SG tubes, evaluation of plant data demonstrates a reduction of a factor of about 1.5 in crack growth rate [38]. For thicker components, initial laboratory testing sponsored by EPRI MRP indicated that there was some evidence for a mitigative effect at low stress intensity factors (SIF) (a factor of improvement of ~ 1.8 for $\text{SIF} \leq 15 \text{ ksi}\sqrt{\text{in}}$) for Alloy 600 but subsequent tests did not show any benefit.

The inconsistent and limited effect of zinc on Alloy 600 and Alloy 182 weld metal tend to suggest that Zn addition alone is not a reliable way to mitigate stress corrosion crack growth in nickel-based alloys [38]. However, it can be part of an overall chemical mitigation strategy involving also optimisation of hydrogen injection [45].

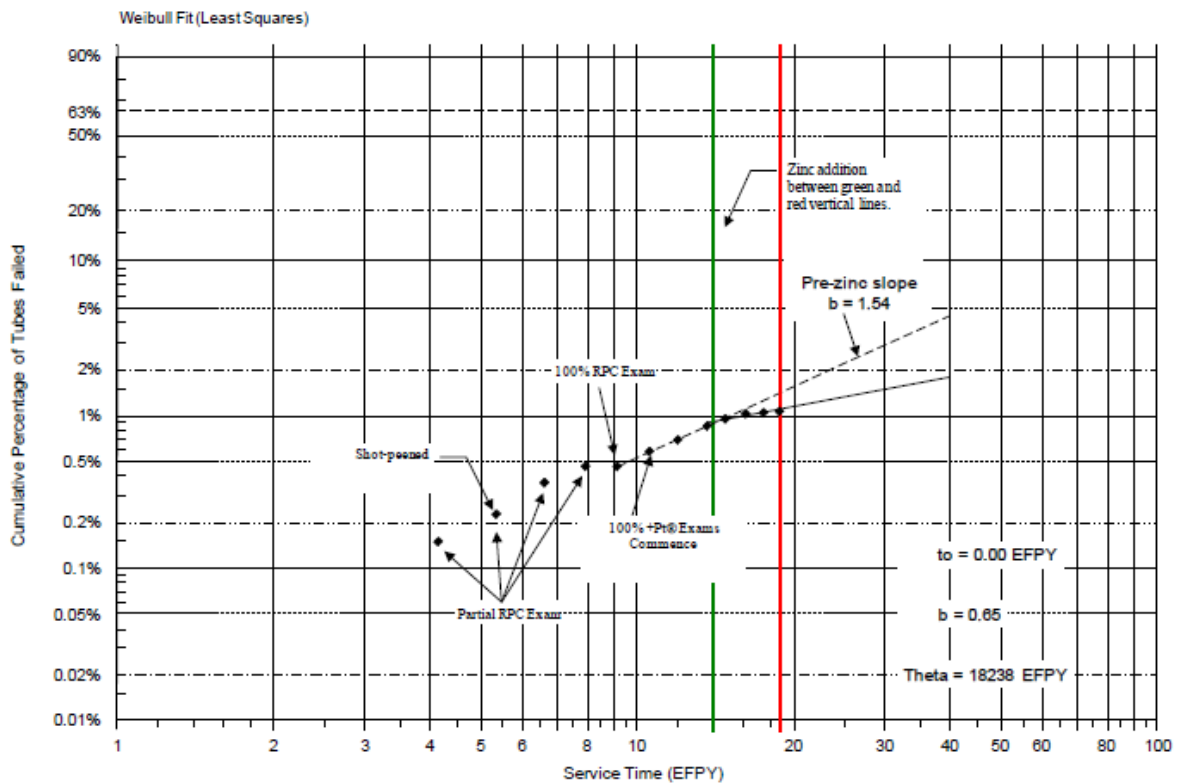


Figure 18 Plant A (all SGs) WEXTEx PWSCC (axial and circumferential)-tubes repaired.

6 Influence of Zn on fuel

6.1 Performance of fuel cladding

PWR feedback has not shown any adverse impact of Zn on fuel integrity [23]. It seems to be well established that zinc has not any impact on fuel cladding corrosion. Independently of duty plant conditions, the oxide thickness measurements carried out in the different alloys (Zircaloy 4, M5, Zirlo) do not reveal any particularity compared with measurements performed before zinc injection start, or on units without zinc injection [46-50]. As an example, data from Tsuruga 2 (Zircaloy 4 cladding) [46], Bugey 2 (Zircaloy 4 cladding) [24] and Sequoyah 2 (M5 cladding) [49] are shown in Figure 19.

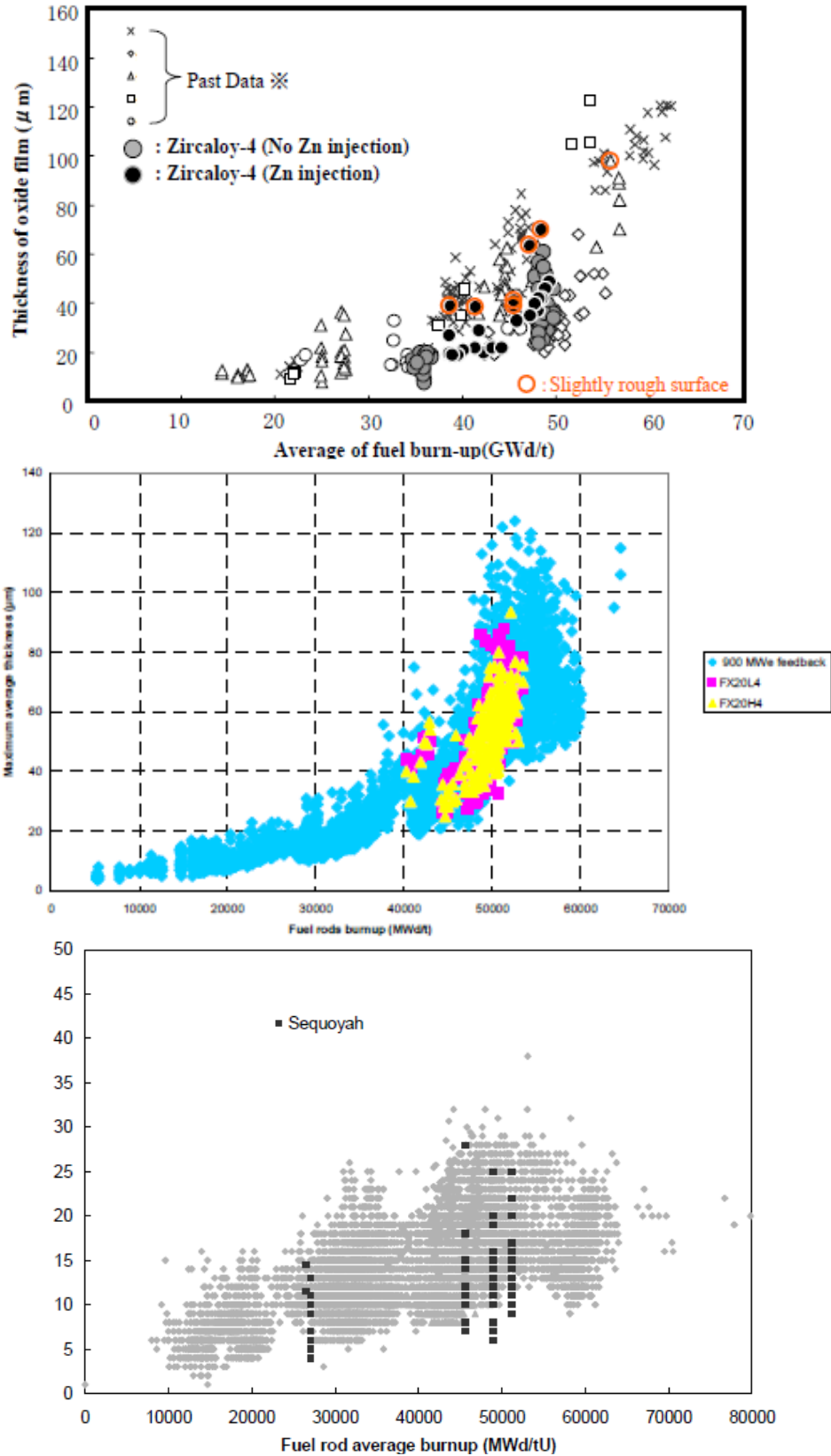


Figure 19 Measurement of Fuel Oxide Thickness at Tsuruga 2 with and without zinc injection (above), Bugey 2 with zinc injection compared with data from 900 MWe units without zinc injection (middle); and SQN-2 results plotted (in black) on the graph of fuel rod average burnup vs. peak oxide layer thickness (in μm) for M5® cladding without zinc injection chemistry (in grey).

6.2 Effect of Zn on fuel crud

Historically, the pH of the reactor coolant in PWRs has been controlled in order to increase the solubility of crud (originally CRUD= Chalk River Unidentified Deposits) when passing through the reactor core for the purposes of reducing crud deposition on the fuel surface. Originally, it was a good concept to mitigate the crud deposition on fuel rods under normal fuel burn-up condition. However, modern PWRs operate under high fuel burnup conditions, so that the fuel that performs with higher duty for longer residence times suffers from unfavourable $\text{pH} < 6.9$ conditions in early stages of operation and undergoes SNB (Sub-cooled Nucleate Boiling) towards the top of the reactor core. Therefore, the amount of crud on fuel rods increases with the increase in the mass of corrosion products from structural materials, and the increase of crud deposition promoted by SNB. The transition to higher duty cores has been accompanied by some crud-related incidents causing anomalous and unanticipated core behaviour in PWRs, fuel integrity problems, and adverse radiological events. In order to mitigate these crud-related incidents, innovative strategies, including zinc addition, have been developed.

The crud investigations and scraping measurements carried out recently [51-55] show that a crud richer in nickel tends to deposit on regions where the SNB is more significant (upper region of assemblies). These deposits seem to accelerate the boron deposition and consequently the development of flux deformation (AOA). In the same way that zinc replaces cobalt on ex-core surface it can be assumed that this substitution can also take place in the crud. The issue is to determine if the “new zinc-crud” is better or worse than the “typical crud”. From scraping investigations, significant modifications of the distribution, structure and composition of the crud introduced by zinc injection have been observed. The “new zinc crud” seems to exhibit the following characteristics:

- it is distributed uniformly along the assemblies contrary to non-zinc deposits which are mostly localized in heated regions.
- its structure is formed by very small particles and there is no evidence of an increase of density in PWR environments.
- The zinc fraction is about 2-7%.

Based on these data, the “zinc crud” has been considered as “benign” [25,56]. It has been recognized that the reduced corrosion rate in the long-term can reduce fuel crud and its possible consequences: Axial Offset Anomalies and/or fuel failures attributed to cladding corrosion. Hence, there are also significant attempts to implement Zn injection as regard of first barrier integrity and power availability of unit’s operation, especially as preventive/mitigation action of future fuel management evolutions.

The possibility of zinc precipitation in fuel crud is a major concern for any zinc injection program. Under typical PWR conditions, the solubility studies [57,58] show that zinc injection does not cause ZnO precipitation on surfaces of primary circuit, in the absence of a concentration mechanism such as SNB and zinc complexation. Therefore, zinc deposition rate is primarily driven by the SNB rate of the core and process of zinc complexation. The SNB mechanism, particularly in conjunction with thick oxide films and crud layers, can cause an increase in the soluble concentration into the pores of the deposit in the boiling area. In fact, the SNB -process provides a mechanism for circulating corrosion products to

concentrate and deposit on the cladding surface. Once porous crud deposits are present, the boiling process also favours the increase in the concentration of any impurity or contaminant in the coolant within the crud layer. While zinc species like zincite (ZnO) and willemite (Zn_2SiO_4) are soluble in the bulk coolant [58], vaporization conditions of the coolant in SNB regions has the possibility to create localized areas where deposition can occur. These potential risks are more significant for plants with high boiling levels (high-duty cores). The High Duty Core Index (HDCI) has been initially used by international community to quantify the boiling risk (Figure 20).

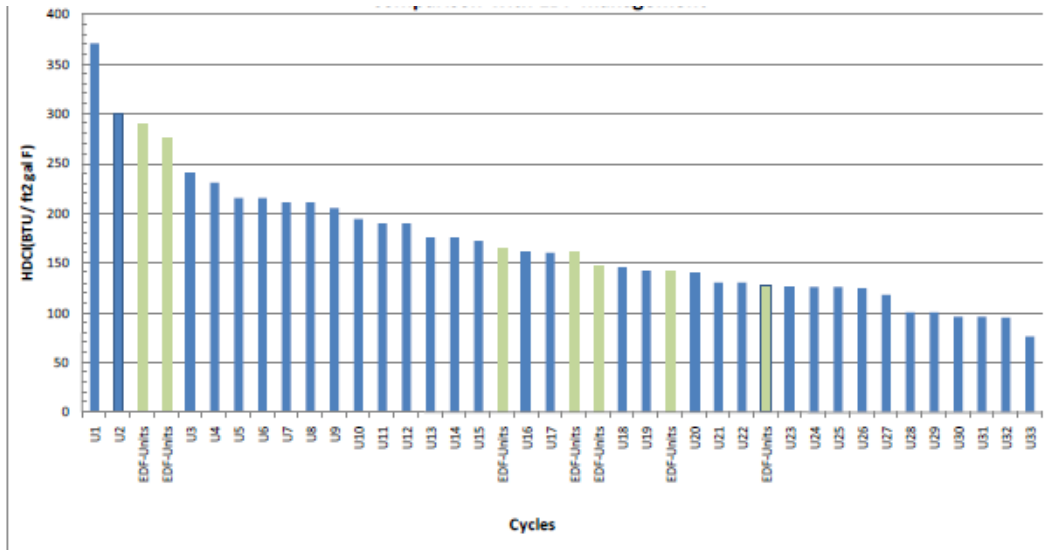


Figure 20 Classification of cycles with zinc injection as a function of HDCI.

However, HDCI is being progressively substituted by the Mass Evaporation Rate (MER) as an indicator for fixing the bounding operating experience of zinc as a function of boiling duty, because of HDCI non pertinence for plants with 14 feet assemblies and the great HDCI variability with temperature (Figure 21).

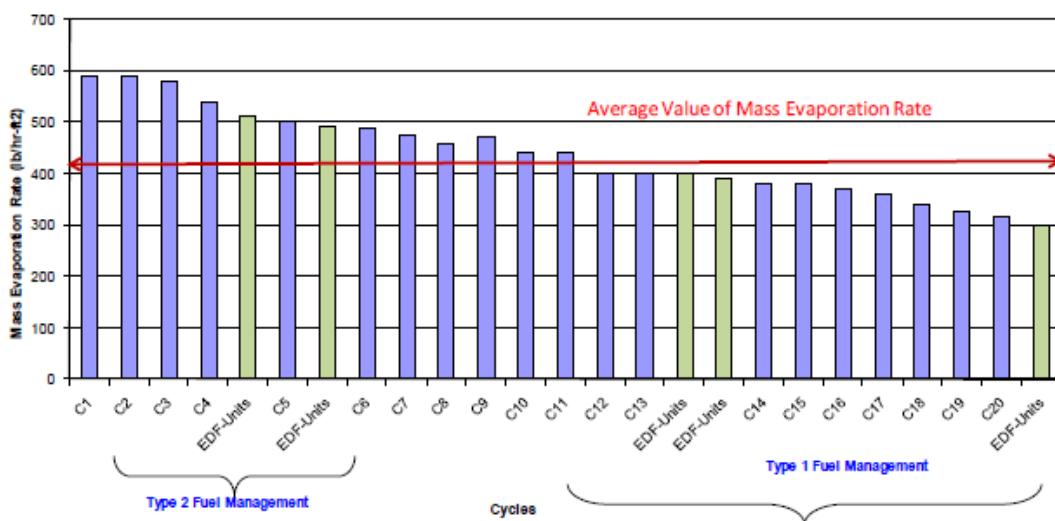


Figure 21 Classification of cycles with zinc injection as a function of Mass evaporation rate

The analysis of Figure 21 has permitted the authors of Ref. 23 to distinguish two categories of units:

- High duty cores (Fuel Management type 2) characterized by $MER >$ average duty level calculated with the available data from units injecting zinc until 2009.
- Low duty cores (Fuel Management type 1) characterized by: $MER <$ average duty level calculated with the available data from units injecting zinc until 2009.

This classification can evolve as a function of the fuel performance progress (enrichment, power, burnup) and core design modifications. It is important to emphasize that MER and HDCI indicators are used to evaluate the core boiling level because it is one of the factors that can enable the crud deposition on fuel cladding. However, a high core boiling level (i.e. high MER and/or HDCI) is not always linked with a high risk of a global core AOA/CIPS. In fact, the development of global deformations depends on the concomitance of several factors: power distribution, boron concentration, core design, corrosion products source term. Therefore, even if the boiling levels of cycles are high, the AOA risk can be compensated by the other factors. For this reason, zinc injection is considered as a preventive mitigation action allowing for reduction of the corrosion product source term and following deposition on the core.

7 Zn injection during HFT

A very recent paper [59] evaluates the effectiveness of starting zinc injection to the RCS with Hot Functional Test (HFT), which was for the first time in the world implemented at Unit 3 of Tomari Nuclear Power Station of Hokkaido Electric Power Co. as a way for radiation exposure reduction. To evaluate the effects on radiation exposure reduction through starting zinc injection to the RCS with HFT, assessment on water chemistry during HFT, implementation of various surface analyses on the SG insert plate dismantled after HFT, assessment on water chemistry during power test, and evaluation of radiation dose rate during each power shutdown have been performed. Comparing the results of analyses and assessment with those of the reference plant Tomari 1, whose water chemistry during test runs was similar to Tomari Unit 3 except zinc injection, the effect due to other measures for radiation exposure reduction and the degree of radiation exposure reduction caused by zinc injection during the first periodical outage at Tomari Unit 3 could be discriminated. The place of zinc injection is illustrated in Figure 22.

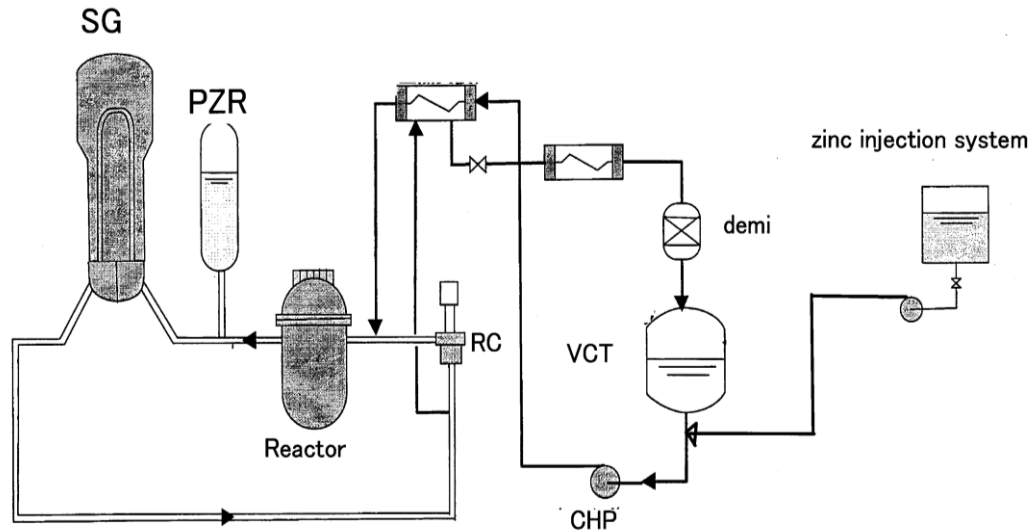


Figure 22 Zinc injection system during HFT at Tomari 3.

In Tomari Unit 3, corrosion mass decreased by 75% compared with Tomari Unit 1, thus corrosion suppression effect of zinc injection was confirmed. The oxide film on the surface of SG insert plate from Tomari 1 and 3 was separated into a deposit layer, outer oxide and inner oxide. Figure 23 shows the element distribution within oxide film, obtained by TEM analysis. The following tendencies were observed: Fe is found to be the major constituent in the deposit layer, Ni concentration was higher in the outer oxide, whereas Cr is the main constituent in the inner oxide. As for zinc, which was thought, among elements analyzed, to be the only one element that was not taken from base material corrosion but from the reactor coolant, aside from showing high concentration in the deposit layer which was nearer to the RCS, Zn concentration is relatively high in the inner oxide. Thus it was supposed that zinc has been incorporated in the initial oxide formed on the material and that a Zn-Cr oxide has been formed by zinc injection starting with the beginning of HFT. In addition, the inner oxide was confirmed to be a poorly crystalline spinel structure. Based on these results, it was presumed that injected zinc is incorporated into inner oxide and stable zinc chromite is formed.

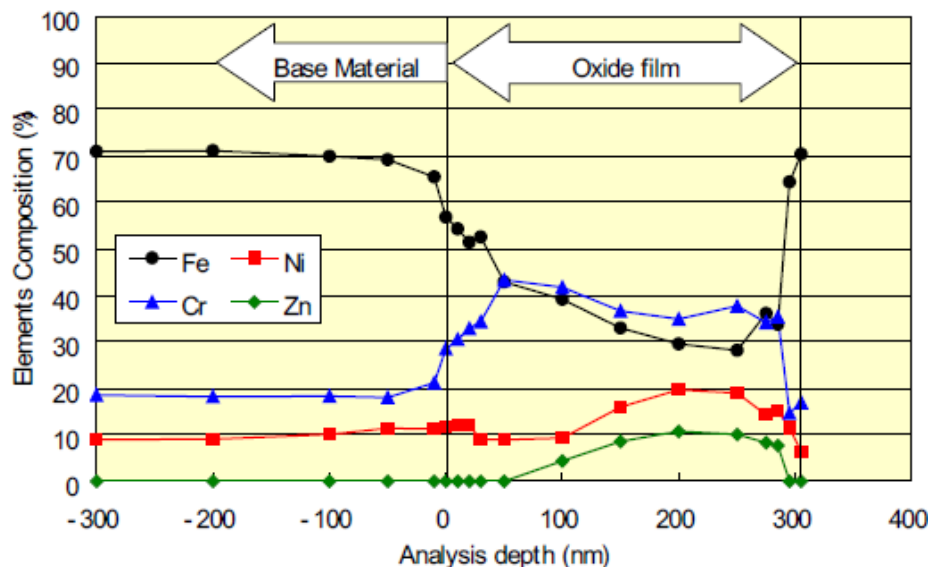


Figure 23 In-depth composition of the oxide on SG material (304SS) from Tomari 3.

The surface dose rate of reactor vessel head and average surface dose rate on main coolant pipe at the end of the first power shutdown test at Tomari Unit 3 were reduced by 40~60% compared with the reference plant. Further, it is expected that the zinc injection effect will be confirmed by the results of the dose rate measurement during the first periodical outage of Tomari Unit 3, scheduled early 2011 [59]. Nevertheless, the first results on the implementation of zinc water chemistry in Hot Functional Test can be deemed satisfactory, at least for this particular plant.

8 Zn injection in WWERs

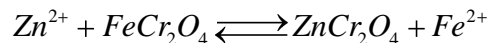
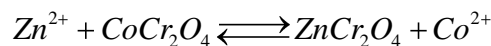
Historically, there are numerous differences between PWR and WWER design that have to a certain extent precluded the possible use of zinc water chemistry in WWERs [60]. Cobalt stellites and nickel alloys, which highly contributed in ^{60}Co and ^{58}Co generation in older PWR plants, were not in use for steam generator tubing and other elements at Russian NPPs. Stress corrosion cracking of steam generator tubing from the primary side and an axial offset anomalies were much less pronounced in WWER plants when compared to PWRs [60]. A high temperature filtration system with total capacity 400-500 m³ per hour at serial VVER-1000 plants (V-320) provides efficient corrosion product removal from primary systems. However, the behavior of zinc in a water coolant has been studied since the mid 1960s at the older Russian design boiling reactors. Zinc presence in water coolant took place due to usage of brass tubing systems for condenser and low pressure heaters [61]. Zinc presence in the coolant up to 0.1 ppm was observed in the beginning of VK-50 operation due to brass selective corrosion and temporary hydrazine injection into turbine condensate. Comprehensive observation of corrosion, deposits and corrosion product behavior in coolant flows showed the dominance of ^{65}Zn and negligible ^{60}Co and ^{58}Co contributions [62, 63]. The generation of ^{60}Co and ^{58}Co was found to be suppressed by zinc presence in primary coolant. These and related studies have demonstrated that implementation of zinc injection into primary coolant could be very effective at the new WWERs from the beginning of plant operation [64]. The protective oxide film allowing minimization of corrosion and radiation fields could be formed during a hot functional test of primary system prior to plant commissioning. The data of radionuclide composition of primary coolant deposit samples in some WWER plants during long-term operation were processed to estimate the effectiveness of zinc injection [16]. Radioactive nuclides ^{60}Co and ^{58}Co were found to account for 55-70% of deposit activity and 73-79% of radiation rate. Thus, removal of ^{60}Co and ^{58}Co from deposits could provide significant reduction of radiation field and occupational exposures also in WWER plants.

Different WWER primary water chemistries were evaluated during experimental loop testing at the LVR-15 reactor under WWER coolant parameters [65]. These were standard WWER primary water chemistry [66], chemistry controls involving gaseous hydrogen injection, high ammonia chemistry and zinc injection. Comparative results revealed the minimum accumulation rate of insoluble corrosion products in case of water chemistry mode with zinc injection. The findings of those studies were taken into account to select an optimum chemical control for some operated and future WWER plants. A pilot zinc injection was scheduled to take place at Bohunice NPP (Slovakia) and Zaporizhe NPP (Ukraine) [64].

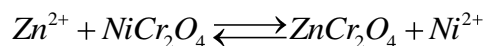
9 Modelling the effect of Zn injection

9.1 Thermodynamic modelling

In order to evaluate the influence of zinc injection on the reduction of radiation buildup and corrosion control, potential-pH diagrams for the Ni-Cr-H₂O, Fe-Cr-H₂O, Co-Cr-H₂O and Zn-Cr-H₂O at 300 °C in the typical PWR primary coolant condition were constructed, and the solubilities of NiCr₂O₄, FeCr₂O₄, CoCr₂O₄ and ZnCr₂O₄ spinel oxides at 573K were also calculated as a function of pH [6,14,15]. In the case of Ni-based alloys (e.g. Alloy 600 and 690), the stable ranges of NiCr₂O₄, CoCr₂O₄ and ZnCr₂O₄, and also an example of potential-pH value in PWR primary coolant are shown in Figure 24 (left). ZnCr₂O₄ is stable with wider potential-pH range in comparison with CoCr₂O₄ and NiCr₂O₄ (the formation of the latter could not be unambiguously proven at nominal PWR conditions by thermodynamic calculations alone). On the other hand, concerning the case of a stainless steel, FeCr₂O₄, CoCr₂O₄ and ZnCr₂O₄ are all stable at nominal PWR conditions (Figure 24, right), but the stability area of zincochromite is the widest. Therefore, in the range that FeCr₂O₄, CoCr₂O₄ and ZnCr₂O₄ stability areas overlap, it is thermodynamically possible that Co and Fe dissolve from the oxide film into the coolant by an exchange reaction with zinc ions:



Further, it is presumed that as the solubility of ZnCr₂O₄ is smaller than that of FeCr₂O₄ in the relevant pH range, general corrosion of stainless steel will be retarded by zinc injection into the coolant [15]. In the case of Ni-based alloys, even if the stability region of nichromite does not extend to the operational range of pH in PWR primary coolants, the authors [15] presume that it can be formed by a small pH excursion. Thus, since the stability of zincochromite is higher, nickel can also be expelled to the coolant at the expense of zinc



Then again, corrosion will be suppressed in the presence of zinc in the coolant since solubility of ZnCr₂O₄ is smaller than that of NiCr₂O₄ in the relevant pH range. Very recent results of thermodynamic calculations have argued that the area of NiCr₂O₄ actually overlaps with the operational pH range in PWR primary coolants [16] or that instead of pure NiCr₂O₄, a mixed spinel of the type Ni_xFe_{1-x}Cr₂O₄ is probably formed on Alloy 690 [21] (Figure 25). This fact points to the uncertainty of thermodynamic calculations when using data on free energies from a range of sources, as well as different algorithms for the calculation of the temperature dependences of heat capacities.

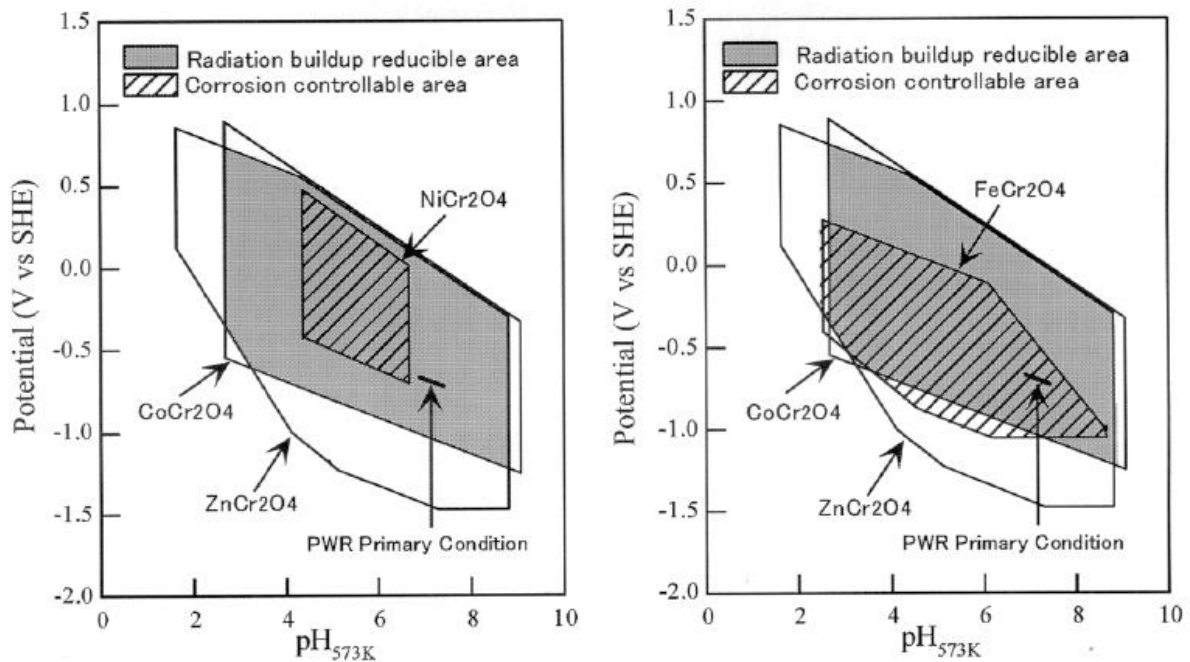


Figure 24 Potential-pH stability areas of spinel oxides presumably formed on nickel-based alloys (left) and stainless steels (right)[15].

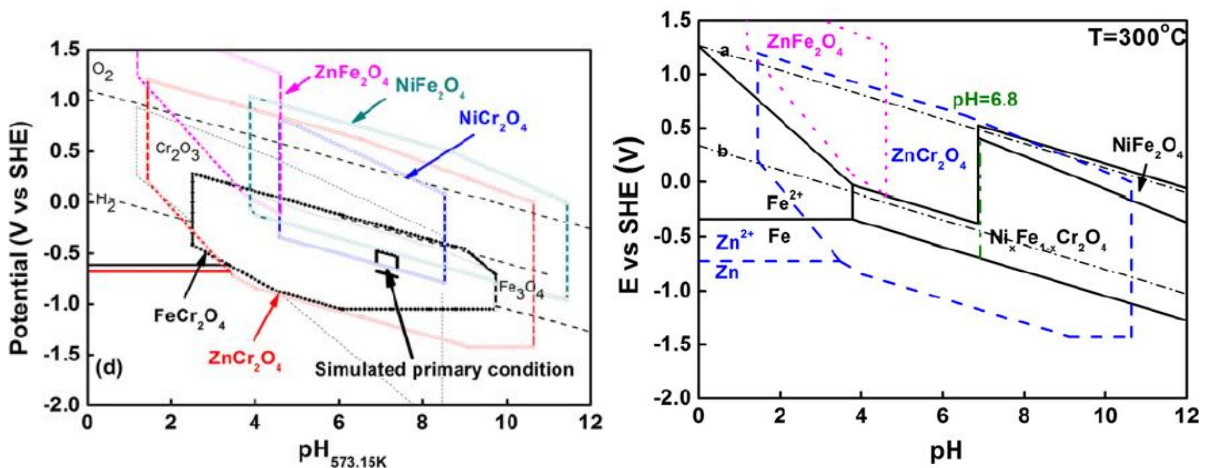


Figure 25 Potential (E)-pH diagrams for the Fe-Cr-Ni-Zn-H₂O system at 300 °C according to Refs. 16 (left) and 21(right).

9.2 Correlations between role of Zn and oxide structure

The oxides formed on the primary circuit construction materials in light water reactors are usually spinels. On carbon steel, the oxide can be either a magnetite or maghemite spinel depending on the reducing or oxidising power of the coolant. On alloyed steels, the alloying elements are incorporated in the growing spinel oxides so that usually an enrichment of Cr is observed in the inner, compact layer, whereas the outer layer is composed mainly of Fe and Ni. Some examples of the structures of spinel oxides containing Zn are collected in Table 2.

A general observation in all the reported zinc tests has been that Zn injection to high temperature water results in thin oxide layers with low visible porosity on new metal surfaces. In addition, the already existing oxide films do not grow in

thickness, partly because corrosion product deposition from the solution is minimal. It has been postulated that zinc somehow decreases the defect concentration in the spinel structure by occupying existing holes in spinel lattice. This should slow down the ion transport through the oxide, leading to a reduced rate of oxide growth and the formation of thinner oxide films [14,67].

It is well known that cations can be placed in the spinel structure either in tetrahedral or octahedral positions. Co and Zn can be considered as dopant ions in the oxide structure. Calculations of displacement energies required to replace one ion with another show that zinc has a very strong stabilisation in tetrahedral sites [68] (Figure 26), and in fact it should be able to displace all other divalent cations from the chromites. This could explain the function of zinc in promoting thinner and more protective oxide films and inhibiting the incorporation of cobalt into the chromium rich oxide film [14,67,69].

Table 2 Examples of typical normal and inverse spinels containing Fe, Cr, Ni, Co, Mn and Zn.

Normal spinel					
Mineral name		Tetrahedral site	Octahedral site	Close-packed	Empty tetrahedral/octahedral sites in a unit cell
Franklinite	ZnFe ₂ O ₄	8 * Zn ²⁺	8 * (Fe ³⁺) ₂	8 * [O ²⁻] ₄	56/16
Danathite	ZnCr ₂ O ₄	8 * Zn ²⁺	8 * (Cr ³⁺) ₂	8 * [O ²⁻] ₄	56/16
	CoCr ₂ O ₄	8 * Co ²⁺	8 * (Cr ³⁺) ₂	8 * [O ²⁻] ₄	56/16
	NiCr ₂ O ₄	8 * Ni ²⁺	8 * (Cr ³⁺) ₂	8 * [O ²⁻] ₄	56/16
Chromite	FeCr ₂ O ₄	8 * Fe ²⁺	8 * (Cr ³⁺) ₂	8 * [O ²⁻] ₄	56/16
	MgCr ₂ O ₄	8 * Mg ²⁺	8 * (Cr ³⁺) ₂	8 * [O ²⁻] ₄	56/16
	MnCr ₂ O ₄	8 * Mn ²⁺	8 * (Cr ³⁺) ₂	8 * [O ²⁻] ₄	56/16
Inverse spinel					
Mineral name		Tetrahedral site	Octahedral site	Close-packed	Empty tetrahedral/octahedral sites in a unit cell
CoFerrite	CoFe ₂ O ₄	8 * Fe ³⁺	8 * (Co ²⁺ + Fe ³⁺)	8 * [O ²⁻] ₄	56/16
Trevorite	NiFe ₂ O ₄	8 * Fe ³⁺	8 * (Ni ²⁺ + Fe ³⁺)	8 * [O ²⁻] ₄	56/16
Magnetite	Fe ₃ O ₄	8 * Fe ³⁺	8 * (Fe ²⁺ + Fe ³⁺)	8 * [O ²⁻] ₄	56/16
	MgFe ₂ O ₄	8 * Fe ³⁺	8 * (Mg ²⁺ + Fe ³⁺)	8 * [O ²⁻] ₄	56/16
Jacobsite	MnFe ₂ O ₄	8 * Fe ³⁺	8 * (Mn ²⁺ + Fe ³⁺)	8 * [O ²⁻] ₄	56/16

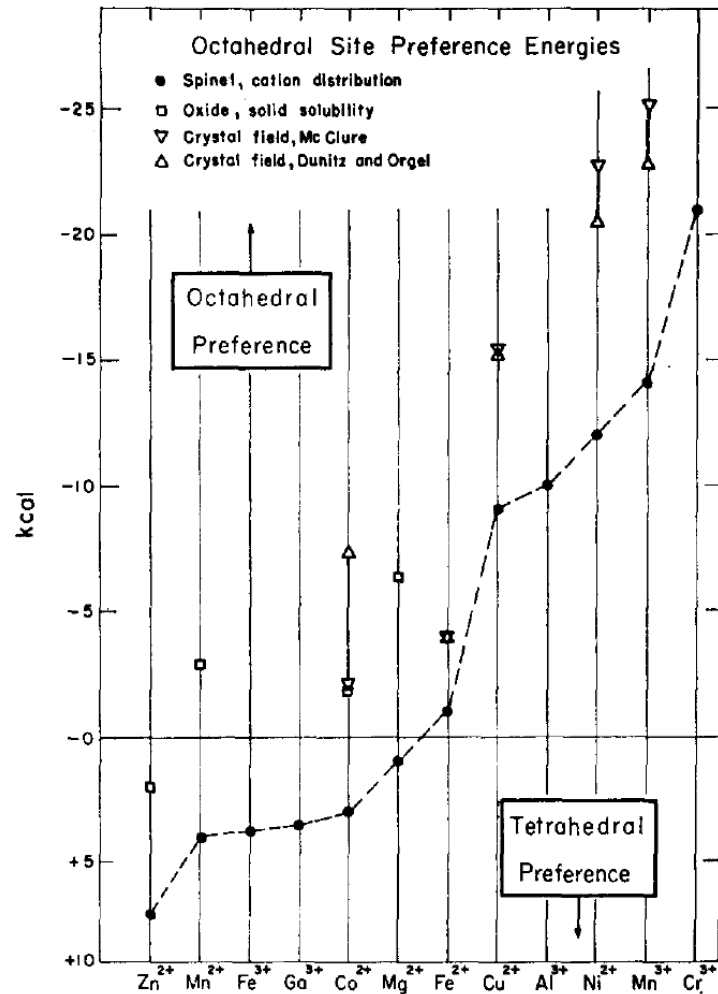


Figure 26 Site preference energy of divalent and trivalent cations in the spinel lattice [68].

9.3 Kinetic modelling

From a kinetic standpoint, the main controlling factor of oxide film growth and metal dissolution rates on stainless steels and nickel-based alloys in PWRs and hence oxide thicknesses and corrosion release are the solid state transport rates within the inner, also called barrier, oxide layer. Models for such transport have been developed for many years, but only recently has the modelling reached a sufficient sophistication to allow a reasonably good quantitative correlation between the modelled values and the growth rates of oxide films on structural materials in real LWR environments. Such a quantitative model, called the Mixed-Conduction Model (MCM) [17,70,71] is described to some detail in the present section of the report. An approach to the growth of the outer and deposited layer crystallites using diffusion formalism is also presented, and the coupling between the models for the compact and porous layers is discussed. In order to treat the incorporation of coolant-originating species, the model is coupled to an adsorption-surface complexation approach which is also briefly described. The physical significance and the relevance of the parameter estimates is described at length in the subsequent section, in which a systematic review of the calculatory results for oxide films formed both in laboratory and during plant operation is presented.

9.3.1 Growth of the inner layer and dissolution of metal through that layer

The MCM approach to the growth of the inner layer is illustrated in Figure 27. Although it has been presumed that Cr and Ni are transported through the oxide via vacancies and Fe via interstitial cation sites, at this point the model does not distinguish between the types of the defects via which the respective metallic constituent is transported through the inner layer of oxide.

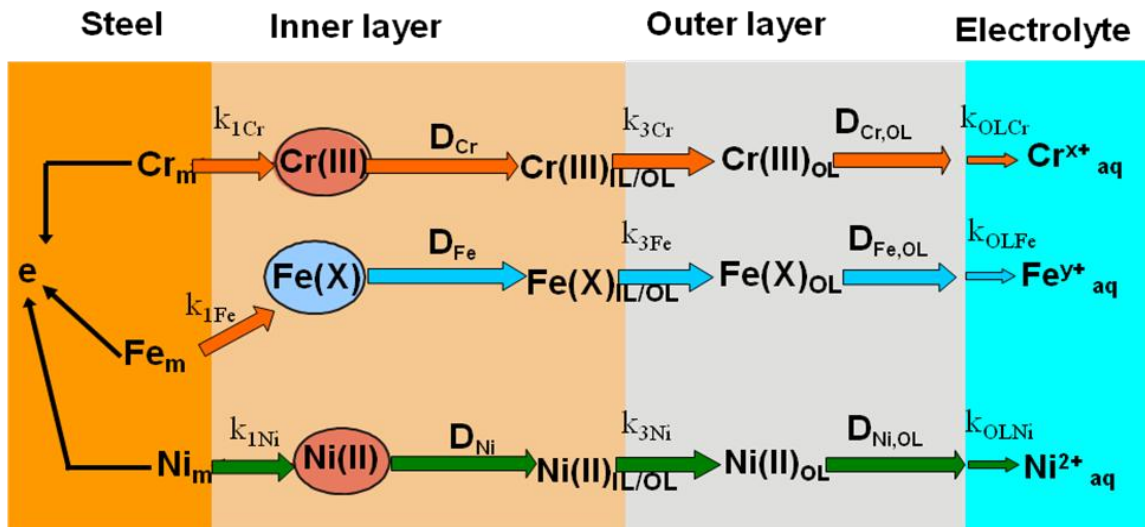


Figure 27 A simplified scheme of the growth of the inner and outer layers of the film formed on a structural material according to the MCM. For details see text.

The depth profile of a metallic oxide constituent $j = \text{Fe, Cr, Ni, etc.}$, can be expressed as the dependence of its molar fraction, $y_j = c_j V_{m,MO}$, on the distance within the inner layer, where c_j is its molar concentration and $V_{m,MO}$ the molar volume of the phase in the layer. The transient diffusion-migration equations for each component read as

$$\begin{aligned}
 \frac{\partial y_{Fe}}{\partial t} &= D_{Fe} \frac{\partial^2 y_{Fe}}{\partial x^2} + \frac{XF\bar{E}D_{Fe}}{RT} \frac{\partial y_{Fe}}{\partial x} \\
 \frac{\partial y_{Cr}}{\partial t} &= D_{Cr} \frac{\partial^2 y_{Cr}}{\partial x^2} + \frac{3F\bar{E}D_{Cr}}{RT} \frac{\partial y_{Cr}}{\partial x} \\
 \frac{\partial y_{Ni}}{\partial t} &= D_{Ni} \frac{\partial^2 y_{Ni}}{\partial x^2} + \frac{2F\bar{E}D_{Ni}}{RT} \frac{\partial y_{Ni}}{\partial x}
 \end{aligned} \tag{1}$$

where X stands for the nominal valence of Fe in the oxide. The boundary conditions at the alloy/film and film/electrolyte interfaces, as well as the initial conditions can be written as

$$\begin{aligned}
 y_{Fe}(x, 0) &= y_{Fe,a}, y_{Cr}(x, 0) = y_{Cr,a}, y_{Ni}(x, 0) = y_{Ni,a} \\
 y_{Fe}(0, t) &= y_{Fe,a}, y_{Cr}(0, t) = y_{Cr,a}, y_{Ni}(0, t) = y_{Ni,a} \\
 y_{Fe}(L_i, t) &= \frac{k_{1Fe} y_{Fe,a}}{V_{m,MO}} \left[\frac{1}{k_{3Fe}} + \frac{RT}{XF\bar{E}D_{Fe}} \right], y_{Ni}(L_i, t) = \frac{k_{1Ni} y_{Ni,a}}{V_{m,MO}} \left[\frac{1}{k_{3Ni}} + \frac{RT}{2F\bar{E}D_{Ni}} \right], \\
 y_{Cr}(L_i, t) &= \frac{k_{1Cr} y_{Cr,a}}{V_{m,MO}} \left[\frac{1}{k_{3Cr}} + \frac{RT}{3F\bar{E}D_{Cr}} \right]
 \end{aligned} \tag{2}$$

where $x = 0$ at the alloy/film interface and $x = L_i$ is the film/coolant or inner layer/outer layer interface, L_i being the inner layer thickness.

9.3.2 Outer layer growth and release kinetics

The outer layer is presumed to grow via the precipitation of material that is dissolved from the substrate through the inner layer of oxide. The growth of this layer is formally treated as a diffusion process in a matrix constituted of the outer layer crystals and the electrolyte in between. Since the outer layer is not continuous, the role of the potential gradient in this layer can be considered negligible with respect to the concentration gradient. Thus, to calculate the depth profile of a certain cation in the outer layer, the following system of equations has to be solved:

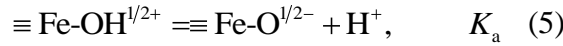
$$\begin{aligned}
 \frac{\partial y_{Fe,OL}}{\partial t} &= D_{Fe,OL} \frac{\partial^2 y_{Fe,OL}}{\partial x^2} \\
 \frac{\partial y_{Cr,OL}}{\partial t} &= D_{Cr,OL} \frac{\partial^2 y_{Cr,OL}}{\partial x^2} \\
 \frac{\partial y_{Ni,OL}}{\partial t} &= D_{Ni,OL} \frac{\partial^2 y_{Ni,OL}}{\partial x^2}
 \end{aligned} \tag{3}$$

The boundary conditions at the inner interface of the outer oxide layer are identical to those used as outer boundary conditions at the inner layer / electrolyte interface (see eqn. (2)), which ensures the continuity of the composition of the whole film. At the outer layer/coolant interface, formal reaction rate constants are introduced: $k_{OL,i}$ ($i=Fe, Cr, Ni$ etc.) and the respective boundary conditions at $x = L_o$, where L_o is the outer layer thickness, are defined as follows

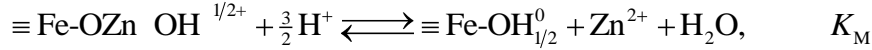
$$\begin{aligned}
 y_{Fe}(L_o, t) &= \frac{k_{3Fe} y_{Fe}(L_i, t)}{k_{OLFe}} \\
 y_{Ni}(L_o, t) &= \frac{k_{3Ni} y_{Ni}(L_i, t)}{k_{OLNi}} \\
 y_{Cr}(L_o, t) &= \frac{k_{3Cr} y_{Cr}(L_i, t)}{k_{OLCr}}
 \end{aligned} \tag{4}$$

9.3.3 Incorporation of solution-originating cations in the oxide

The first step in the interaction between an oxide and a solution-originating cation is adsorption on the outer surface of the oxide, which is treated using the surface complexation approach. The surface hydrolysis of an oxide in PWR coolant conditions is described in terms of the 1-pK surface complexation model [72]



Correspondingly, the interaction of a coolant-originating cation, e.g. Zn^{2+} with the oxide surface is written as



In order to predict quantitatively the depth profile of a solution-originating cation that is incorporated into the inner layer, the associated diffusion-migration equation for the non-steady state transport of that cation, e.g. for Zn

$$\frac{\partial c_{\text{Zn}}}{\partial t} = D_{\text{Zn}} \frac{\partial^2 c_{\text{Zn}}}{\partial x^2} - \frac{2F\vec{E}D_{\text{Zn}}}{RT} \frac{\partial c_{\text{Zn}}}{\partial x} \quad (6)$$

is added to the system of equations (1) and the extended system is solved subject to the boundary conditions (2). The boundary condition at the inner layer/outer layer interface is given by the enrichment factor $K_{\text{enr,Zn,i}}$ defined as the ratio between the concentration of Zn at that interface and the Zn concentration in the water: $y_{\text{Zn}}(L_i, t) = K_{\text{enr,Zn,i}} c_{\text{Zn}}(\text{sol})$. A reflective boundary condition is used for Zn at the alloy / inner layer interface since there is usually no Zn present in the alloy substrate.

Within the frames of the formal model for the outer layer growth, the depth profile of e.g. Zn in the outer layer is calculated by solving the system of equations (3) extended with a corresponding equation for Zn:

$$\frac{\partial y_{\text{Zn,OL}}}{\partial t} = D_{\text{Zn,OL}} \frac{\partial^2 y_{\text{Zn,OL}}}{\partial x^2} \quad (7)$$

The boundary condition at the outer layer/water interface is set by the corresponding enrichment factor for the respective component at that interface, e.g. for Zn: $y_{\text{Zn}}(L_o, t) = K_{\text{enr,Zn,o}} c_{\text{Zn}}(\text{sol})$.

9.3.4 Comparison with experimental data

9.3.4.1 Effect of exposure time and Zn addition on the kinetic parameters of film growth on AISI 304 stainless steel

The experimental and calculated depth profiles of the molar fractions of Fe, Cr and Ni in the oxides formed on AISI 304 stainless steel in simulated PWR water without Zn addition at 260°C for 5000 and 10 000 h [11] are shown in Figure 28. The corresponding profiles obtained in simulated PWR water with the addition of 30 ppb of Zn after 1000 and 10 000 h of oxidation are presented in Figure 29 [12]. The oxides formed in the presence of Zn are significantly thinner than those in the absence of Zn, and significant amounts of Zn are incorporated in the outer part of the inner layer. The profile of Zn in the inner layer follows to a certain extent that of Cr, and the enrichment of Cr in the Zn-doped inner layers is more significant than that in the inner layers formed in the absence of Zn. The outer layer is significantly thinner than the inner layer in the presence of Zn, especially for a 10 000 h of exposure. The calculated profiles (shown in the figures with solid lines)

match sufficiently well the experimental ones, except for the profile of Zn in the vicinity of the alloy/inner layer interface. This could be due to sputtering effects since no Zn is expected to be present in the base alloy. The values of the kinetic parameters calculated from the simulation are shown in Figure 30 (rate constants at the alloy/inner layer and inner layer/electrolyte interfaces) and Figure 31 (diffusion coefficients in the inner layer and formal diffusion coefficients of the growth of the outer layer, respectively).

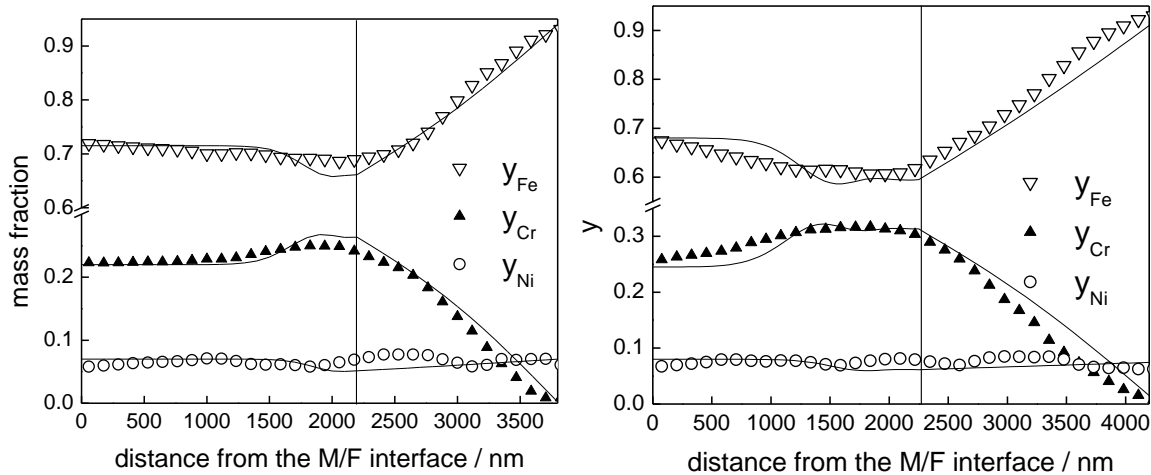


Figure 28 Experimental (points) and calculated (solid lines) XPS depth profiles of the mass fractions of Fe, Cr, and Ni in the films formed on AISI 304 during a 5000 h (left) and 10 000 h (right) exposure to a simulated PWR water at 260 °C. The inner layer / outer layer boundary indicated with a vertical line.

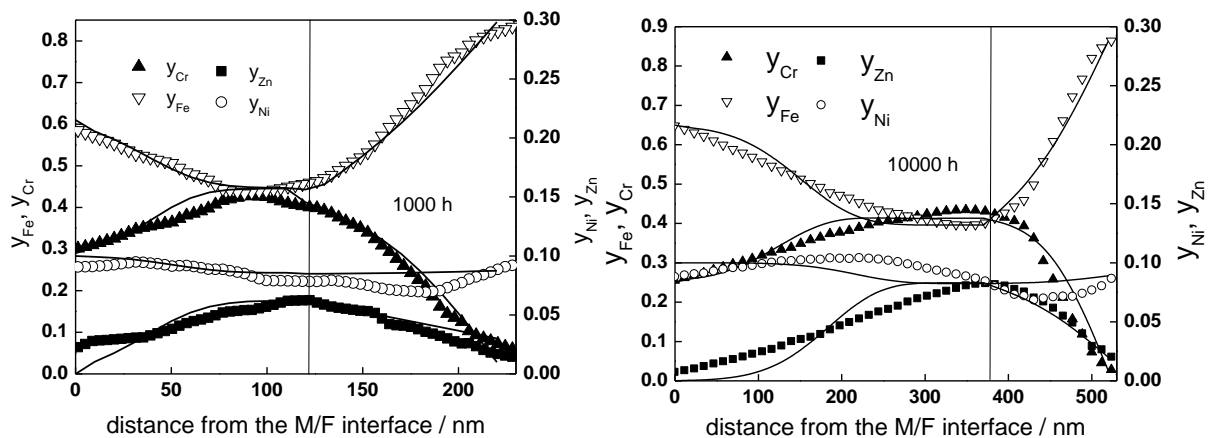


Figure 29 Experimental (points) and calculated (solid lines) XPS depth profiles of the mass fractions of Fe, Cr, Ni and Zn in the films formed on AISI 304 during a 1000 and 10,000 h exposure to a simulated PWR water with the addition of 30 ppb Zn at 260 °C. The inner layer / outer layer boundary indicated with a vertical line.

The effect of Zn on the kinetic and transport parameters is significant, especially on the diffusion coefficients in the inner layer and the formal diffusion coefficients depicting the growth of the outer layer of oxide. In other words, when the film grows in an electrolyte containing Zn, the transport rate in the inner layer of oxide has been reduced by a factor of 3-4, and the growth of the outer oxide is almost totally suppressed, especially for longer oxidation times (Figure 31).

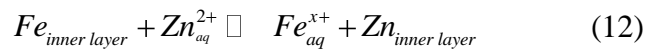
The decreasing effect of Zn on the kinetics of the interfacial reactions is comparatively weaker, with one notable exception – in solutions containing Zn, the rate constant of Fe dissolution from the inner layer is somewhat larger than that in electrolytes without Zn addition (Figure 30). It is tempting to assume that Zn is substituted for divalent Fe, thus expulsing the latter from the oxide, as already discussed by several authors [6,13,73]. The following line of reasoning is proposed to explain these observations. If the incorporation of Zn at the inner layer/electrolyte interface occurs via filling of available empty cation interstices V_i and/or cation vacancies V_M^m :



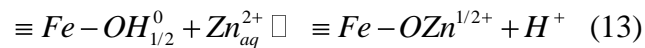
then the concentration of these defects at the interface will decrease. In order their steady-state concentration to be maintained, an additional amount of Fe (the main element of the alloy) has to dissolve according to the reactions



According to the model described above, the sum of the rate constants of the reactions (10) and (11) is equal to the rate constant k_{3Fe} , which is observed to increase with the addition of Zn to the electrolyte. Further incorporation of Zn in the bulk of the inner layer will lead to a decrease of the concentration of defects, and also their mobilities, within the oxide. This in turn explains the much smaller values of the diffusion coefficients of inner layer constituents when the film is grown in solutions that contain Zn. The sum of the reactions (8)-(11) can be written as an equilibrium exchange between a Fe cation in the inner layer of oxide and a Zn aquoion in the electrolyte, in analogy with what has been proposed in Ref.13:



Alternatively, the first step of Zn incorporation in the oxide can be written as a surface complexation reaction, as outlined above



The equilibrium constant of this reaction on magnetite has been estimated to be 41.7 at 280°C using the constant capacitance model to quantitatively interpret high-temperature titration data on magnetite surfaces in simulated PWR water [74]. The equilibrium constant can be also estimated from the present results using data on the molar fractions of Zn and Fe at the inner layer/electrolyte interface (Figure 29), the surface site concentration on magnetite estimated earlier from titration data (1.75×10^{-10} mol cm⁻²) and the speciation of soluble Zn in the electrolyte calculated using literature data [74]. A value of 60±10 is obtained, in reasonable agreement with the surface complexation calculations. It can be concluded that the first step of Zn incorporation into the oxide is described adequately by the surface complexation

model and equation (13). It is worth noting that recent estimates of the surface site concentration and the point of zero charge of trevorite in hydrothermal conditions [75] demonstrate that the above interpretation remains valid also for the interaction of Zn with trevorite.

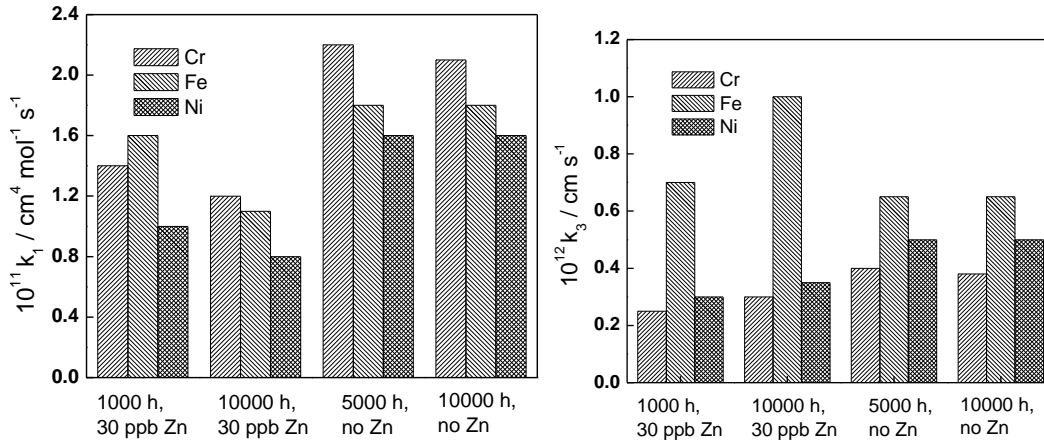


Figure 30 Dependence of the rate constants for inner layer constituents at the alloy/inner layer (left) and inner layer/electrolyte (right) interfaces on time of exposure and Zn addition.

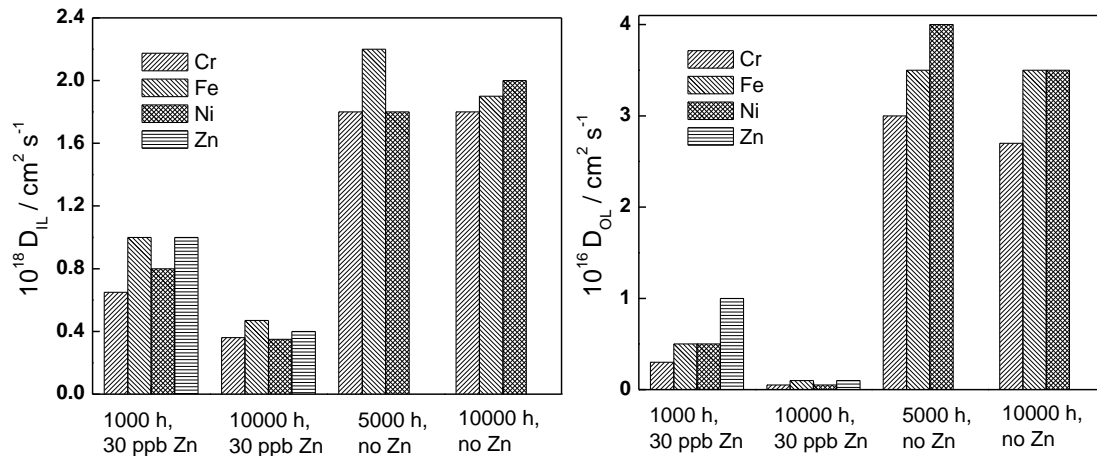


Figure 31 Dependence of the diffusion coefficients of inner layer constituents (left) and formal diffusion coefficients depicting the growth of the outer layer (right) on time of exposure and Zn addition.

9.3.4.2 Effect of Zn on in-reactor Co incorporation in the oxide on stainless steel

The effect of Zn on the incorporation of Co from the coolant into the oxides formed on stainless steels and nickel-based alloys has been thoroughly investigated by the Halden Reactor project [76,77]. Both fresh and preoxidised samples have been exposed to PWR in-plant conditions (soluble Zn either 0 or ca. 50 ppb), the duration of each exposure phase being ca. 100 Effective Full Power Days (EFPD). The SIMS depth profiles for Fe, Cr, Ni, Co, Mn and Zn in the films obtained after the first and third exposure phase on fresh AISI 304 sample in the presence of 50 ppb Zn in the water are shown in Figure 32 together with the profiles calculated using the present model. The kinetic and transport parameters estimated from the calculation are collected in Figure 33. The following conclusions can be drawn on the basis of the parameter values:

- The set of parameters used to simulate the in-reactor film growth and restructuring on AISI 304 is fully compatible with that used for the simulation of

the growth and restructuring on the same steel in laboratory conditions (see previous paragraph). This demonstrates the feasibility of the present model also for the interpretation of in-reactor data.

- The equilibrium constant of Co incorporation via a reaction analogous to (13) was estimated to be close to 1, which agrees by order of magnitude with the value calculated on the basis of high-temperature titration data and the surface complexation model [74], whereas the corresponding value for Zn incorporation was again of the order of 50, confirming the earlier calculations and demonstrating once again the higher affinity of Zn towards the surface oxide.
- The main effects of Zn are on the values of the diffusion coefficients in both layers and to a certain extent on the values of the rate constants at the outer interface. This can be interpreted as a modification of both the oxide surface and the bulk oxide by Zn addition.
- Oxide growth/restructuring and incorporation of Co in the oxide are retarded by Zn incorporation. This could be related to the formation of new Zn-containing phases in both the inner and outer layers, as discussed also by other authors [6,13,15,16].

SIMS depth profiles for Fe, Cr, Ni, Co and Zn in the films obtained after in-reactor exposure of a preoxidised AISI 304 sample to PWR water in the presence or absence of Zn are shown in Figure 34 together with the corresponding profiles calculated by the model. The kinetic and transport parameters estimated from the calculation are collected in Figure 35. On comparing the parameter values for the fresh and preoxidised samples, it can be concluded that:

- Incorporation of Zn in already existing oxides is slower, and the layer restructuring is less pronounced. The diffusion coefficients in the inner layer formed in the presence of Zn on the preoxidised samples are ca. 50% lower than those formed on the fresh sample, and when the Zn-doped oxide is once again exposed to Zn-free PWR water, their initial values are restored. This means that the incorporation of Zn in pre-existing oxides is to a great extent reversible, thus less effective in suppressing further oxide growth and incorporation of solution-originating Co.
- There is no appreciable difference between the values of the apparent diffusion coefficients in the outer layer in both cases, with the notable exception of the diffusion coefficient for Co - when Zn is added, $D_{Co,OL}$ decreases to a half of its value before Zn addition. Thus Zn addition suppresses incorporation of Co in the outer layer as well.
- The value of the rate constant k_{3Fe} is once again much higher in the presence of Zn which could be interpreted as if the exchange reaction of Zn for Fe being efficient enough for preoxidised samples as well and its mechanism being essentially unaltered.

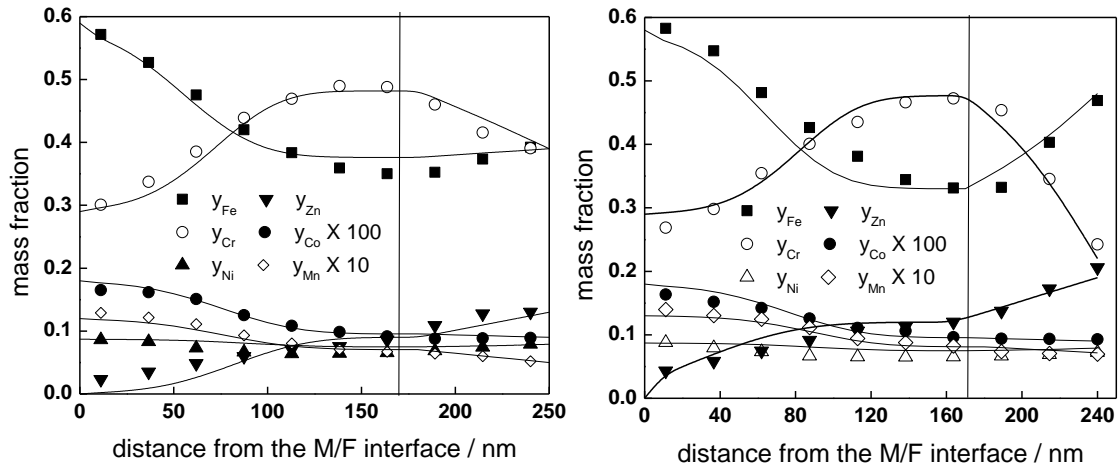


Figure 32 Experimental (points) and calculated (solid lines) depth profiles of the mass fractions of Fe, Cr, Ni, Co, Mn and Zn in the films formed on AISI 304 after the exposure to ca. 100 and 300 EFPD (125 and 336 days) in the Halden Reactor, PWR coolant conditions. The inner layer / outer layer boundary indicated with a vertical line. Experimental data taken from Refs 72-76.

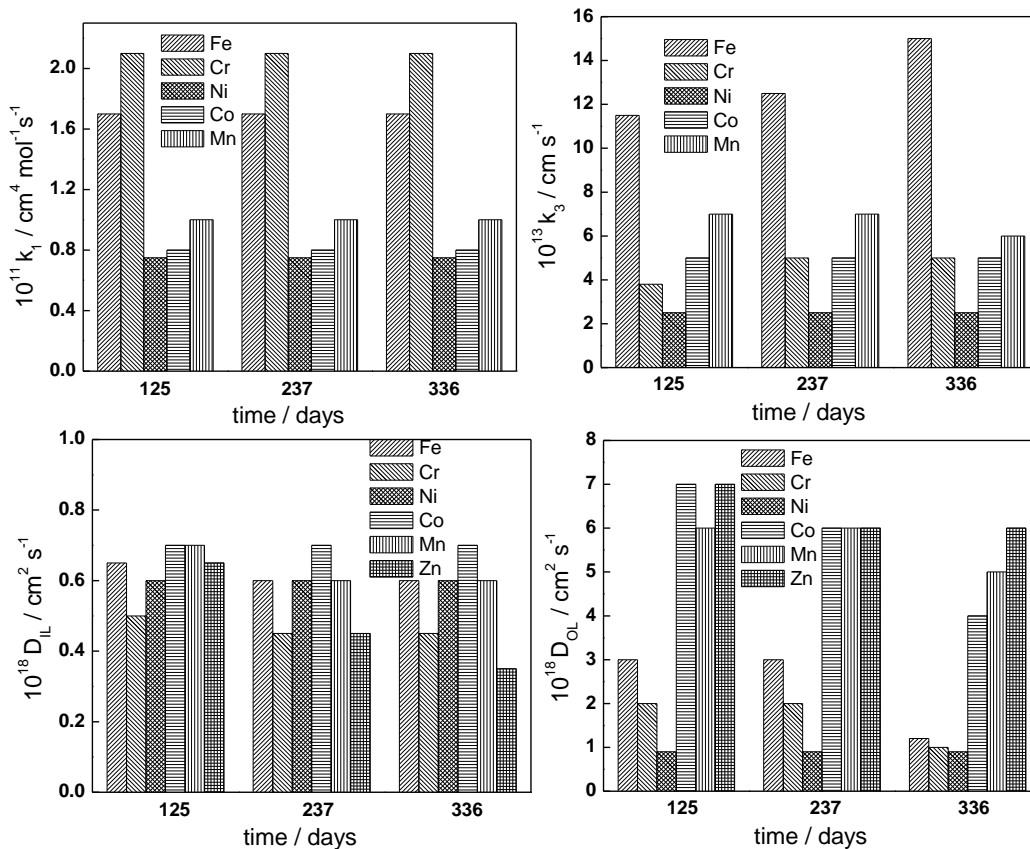


Figure 33 Dependence of the rate constants at the steel/inner layer interface (above left), the inner layer/electrolyte interface (above right), diffusion coefficients of inner layer constituents (below left) and formal diffusion coefficients depicting the growth of the outer layer (below right) on time of exposure. 50 ppb Zn added from the beginning of exposure.

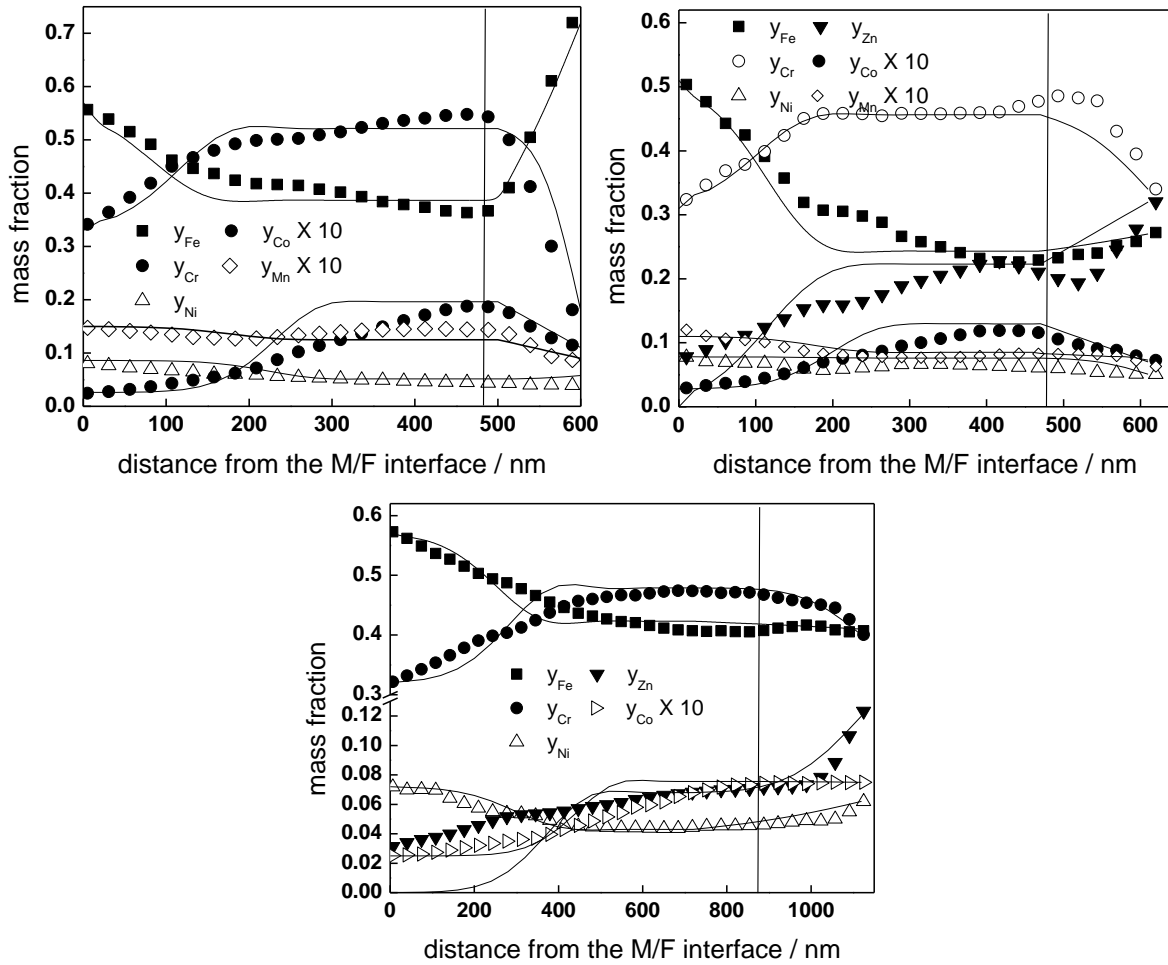
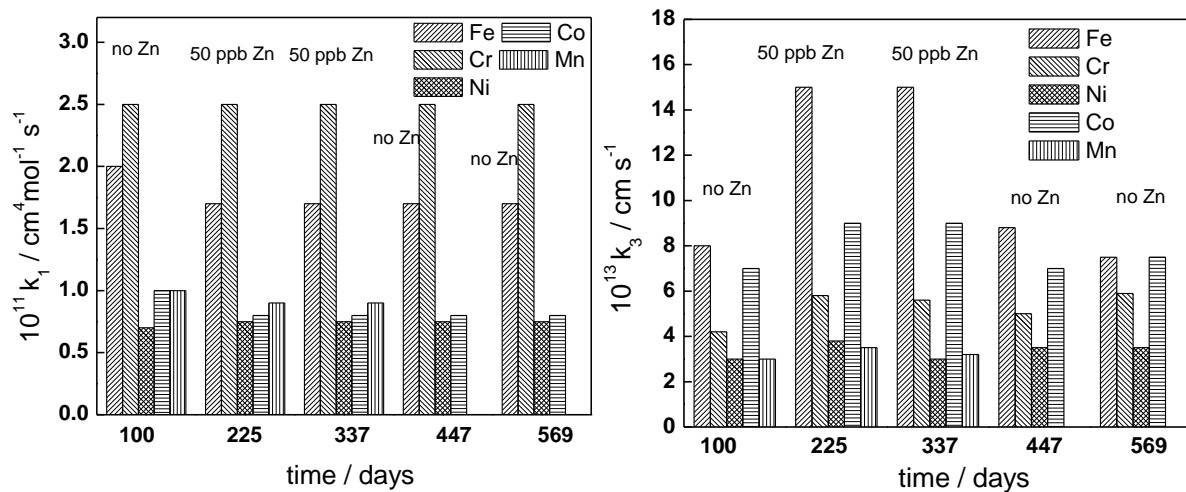


Figure 34 Experimental (points) and calculated (solid lines) depth profiles of the mass fractions of Fe, Cr, Ni, Co, Mn and Zn in the films formed on AISI 304 during a 100 day exposure with no Zn addition (above left), followed by a 237 day exposure to 50 ppb Zn (above right) and another 230 day exposure with no Zn addition (below). The inner layer / outer layer boundary indicated with a vertical line.



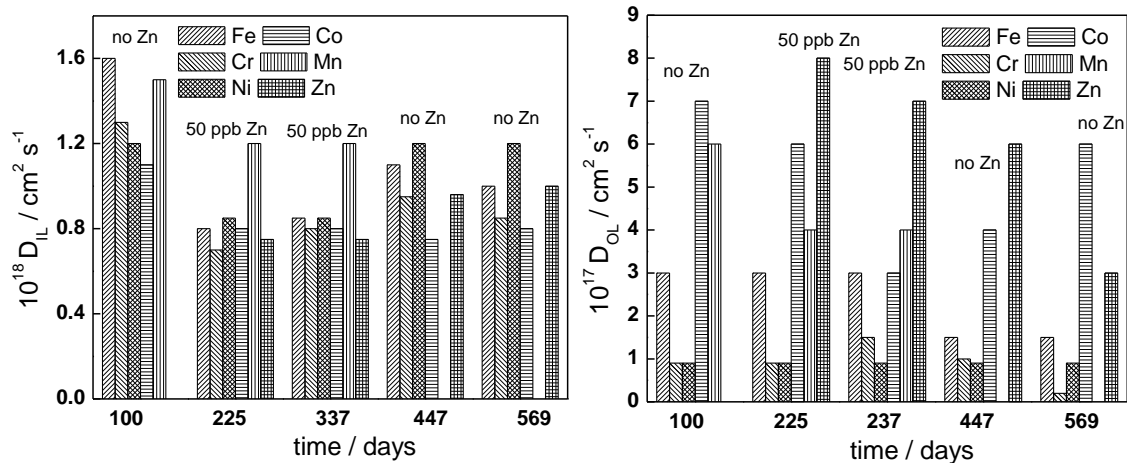


Figure 35 Dependence of the rate constants at the steel/inner layer interface (above left), the inner layer/electrolyte interface (above right), diffusion coefficients of inner layer constituents (below left) and formal diffusion coefficients depicting the growth of the outer layer (below right) on time of exposure of AISI 304 to PWR water. Successive periods without and with Zn as indicated.

Further proof for the validity of the model comes from Figure 36, in which the inner layer thicknesses for the oxides formed on AISI 304 in both simulated and in-reactor PWR environment with or without Zn addition are compiled as depending on exposure time. In the figure, experimentally determined thickness values are compared with the thickness calculated according to the relationship proposed within the frames of the MCM [71]

$$L(t) = L(t=0) + \frac{1}{b} \ln \left[1 + V_{m,MO} (k_{1,Cr} y_{Cr,a} + k_{1,Fe} y_{Fe,a} + k_{1,Ni} y_{Ni,a}) b e^{-bL(t=0)t} \right], b = \frac{3\alpha_1 F \bar{E}}{RT} \quad (14)$$

subject to the assumption that the transfer coefficients for all the three reactions at the metal film interface are similar and equal to α_1 and the values of the rate constants are taken from Figure 30, Figure 33 and Figure 35. Notwithstanding the fact that the compilation of data is stemming from exposure to slightly different experimental conditions, the solid lines shown in Figure 36 demonstrate the fair agreement between the experimentally estimated thicknesses and model predictions, which is encouraging taking into account the fact that no further adjustment has been made.

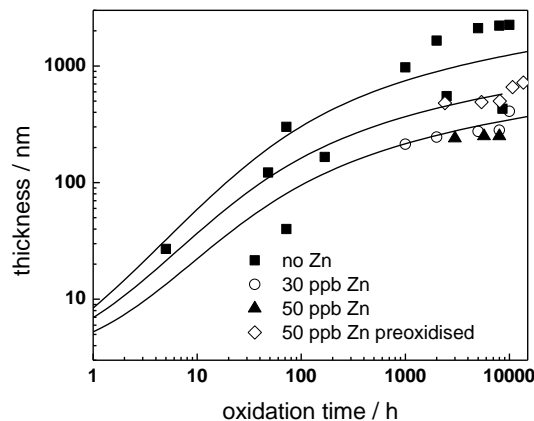


Figure 36 Inner layer thickness vs. time data for AISI 304 in simulated and in-reactor PWR water with or without Zn addition at 260-300 °C (symbols) and calculated curves according to the model (solid lines).

9.3.4.3 Effect of exposure time and Zn addition on the kinetic parameters of film growth on nickel-based alloys

XPS depth profiles for the oxides on Alloy 600 stemming from experiments in simulated PWR water with and without the addition of 30 ppb of soluble Zn at 260°C [18,19] are presented in Figure 37 and Figure 38, respectively. The parameters used to reproduce the experimental profiles are collected in Figure 39. Concerning in-reactor exposure, SIMS depth profiles for Fe, Cr, Ni, Co and Zn in the films obtained on a fresh Alloy 690 sample after the first and third exposure phase of the Halden reactor project experiment discussed above in the presence of 50 ppb Zn in the water are shown in Figure 40 together with the profiles calculated using the present model. The kinetic and transport parameters estimated from the calculation are collected in Figure 41 and Figure 42.

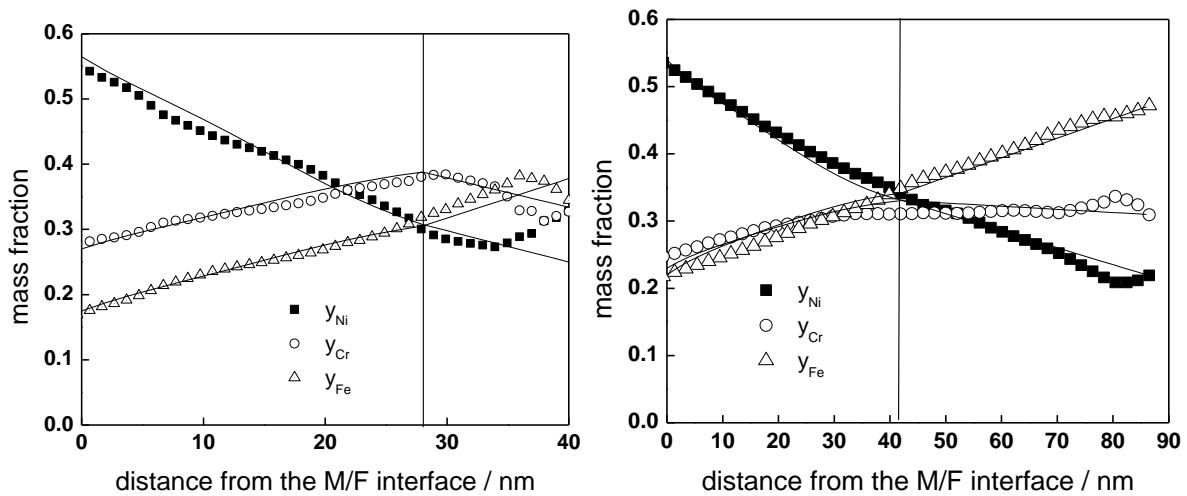


Figure 37 Experimental (points) and calculated (solid lines) depth profiles of the mass fractions of Fe, Cr, and Ni in the films formed on Alloy 600 in simulated PWR water for 5000 h (left) and 10000 h (right). The inner layer / outer layer boundary indicated with a vertical line.

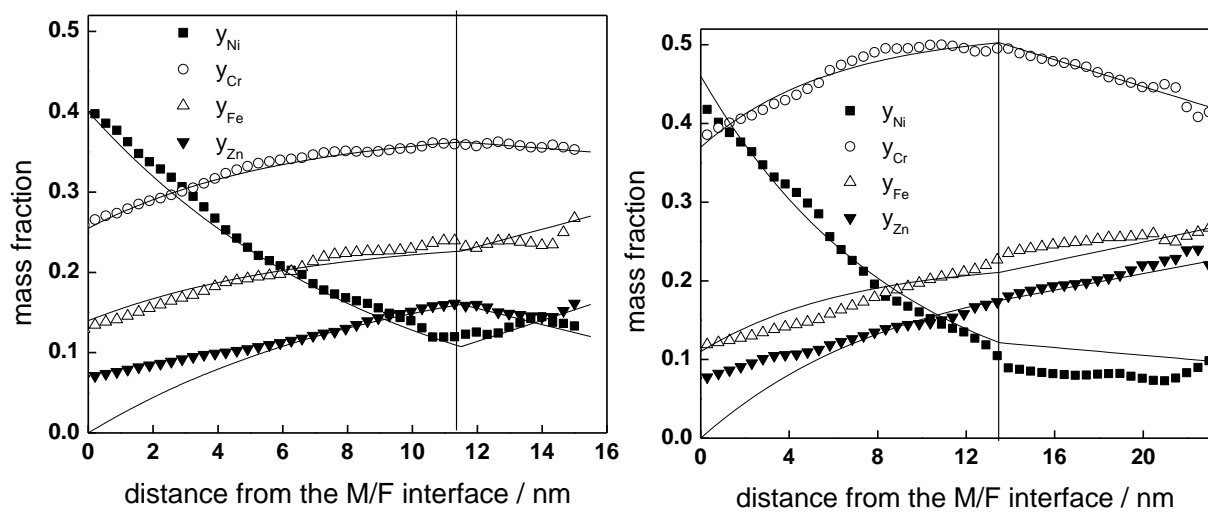


Figure 38 Experimental (points) and calculated (solid lines) depth profiles of the mass fractions of Fe, Cr, Ni, and Zn in the films formed on Alloy 600 in simulated PWR water with 30 ppb Zn for 5000 h (left) and 10000 h (right). The inner layer / outer layer boundary indicated with a vertical line.

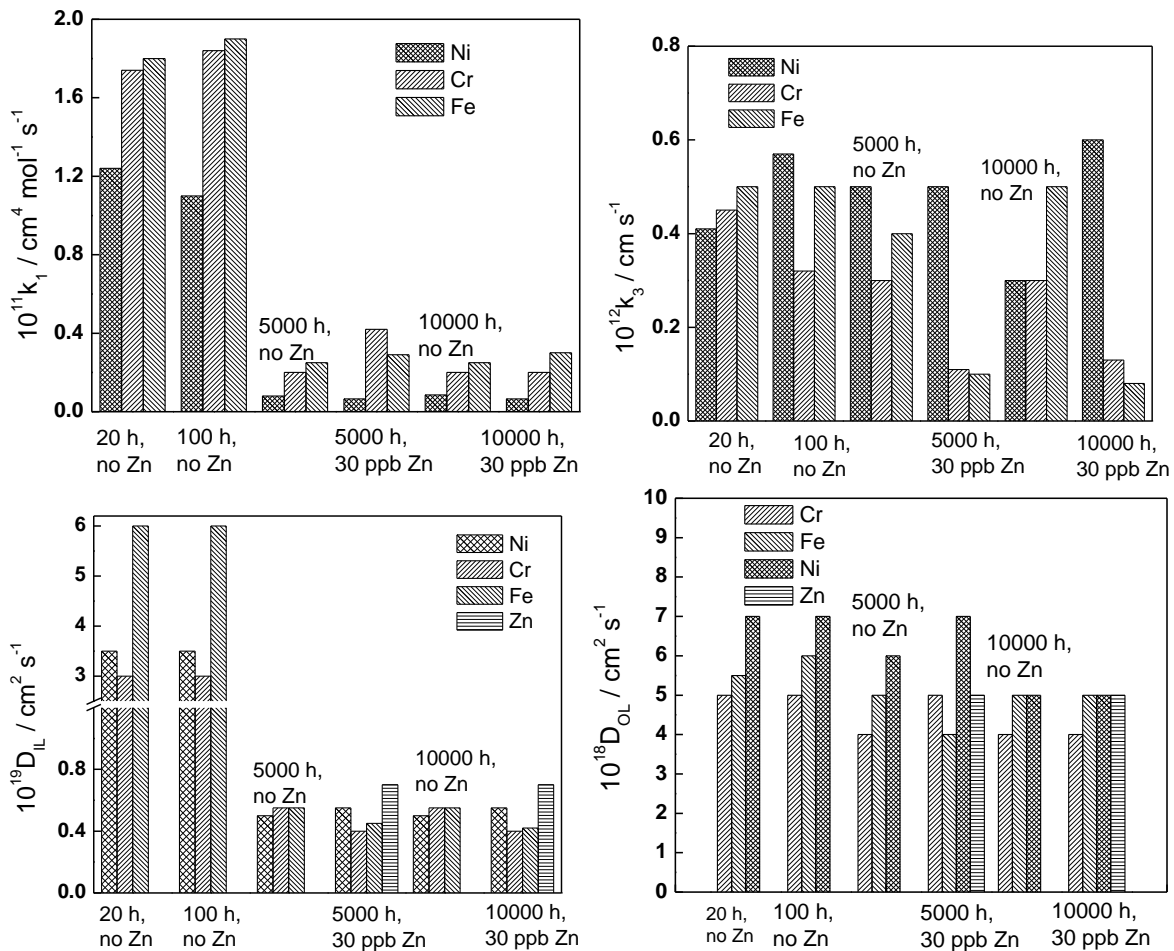


Figure 39 Dependence of the rate constants at the alloy 600 / inner layer interface (above, left), inner layer/electrolyte interface (above, right), diffusion coefficients of inner layer constituents (below left) and formal diffusion coefficients for the growth of the outer layer (below right) on time of exposure to simulated PWR water with or without Zn addition.

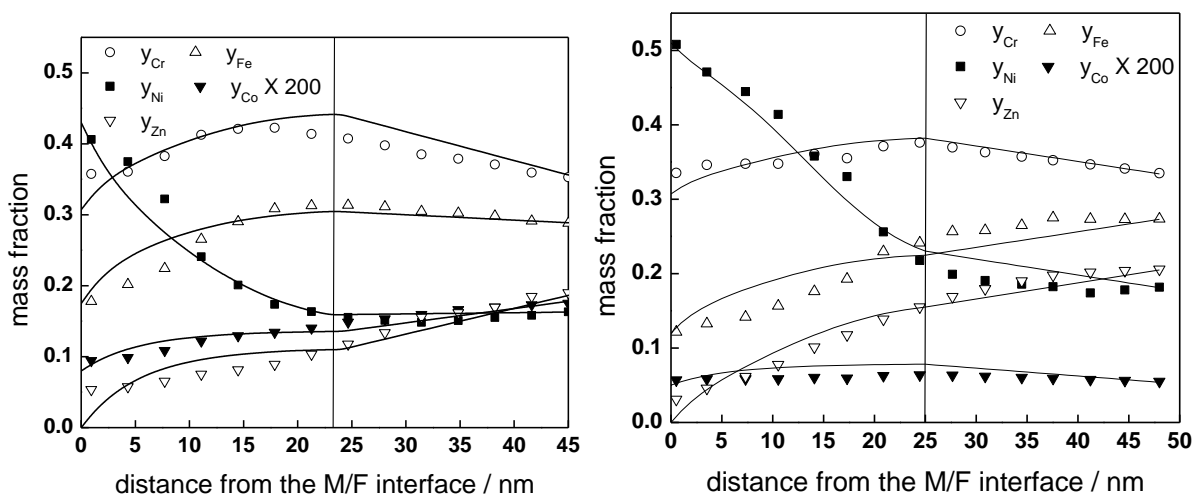


Figure 40 Experimental (points) and calculated (solid lines) depth profiles of the mass fractions of Fe, Cr, Ni, Co and Zn in the films formed on Alloy 600 during the first and second exposure to ca. 100 Effective Power Days in the Halden Reactor, PWR coolant conditions. The inner layer / outer layer boundary indicated with a vertical line.

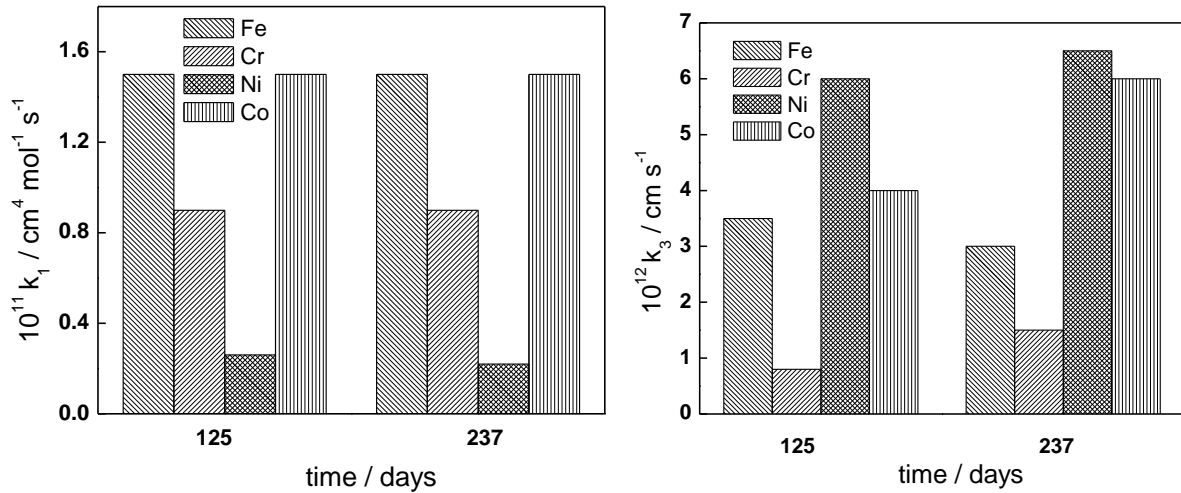


Figure 41 Dependence of the rate constants at the Alloy 690 / inner layer interface (left) and the inner layer/electrolyte interface (right) on the time of exposure of Alloy 690 to PWR water containing 50 ppb of Zn.

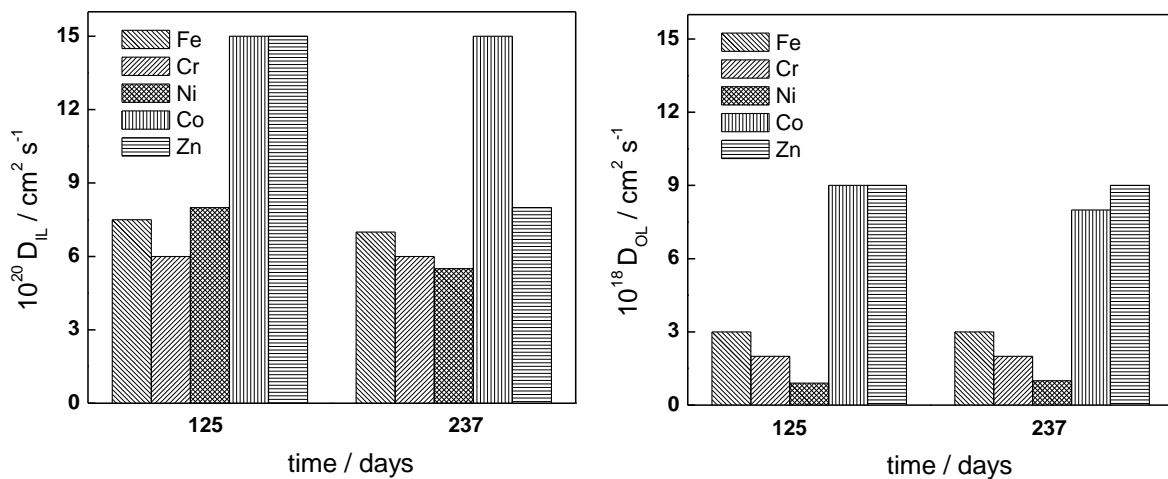


Figure 42 Dependence of the diffusion coefficients of inner layer constituents (left) and formal diffusion coefficients for the growth of the outer layer (right) on the time of exposure of Alloy 690 to PWR water with 50 ppb of Zn.

Concerning the effect of Zn on the oxide growth and restructuring, it can be stated that the effect is much smaller on the oxides formed on Ni-based alloys than on those formed on stainless steels, even if the amounts of incorporated Zn especially in the outer part of the inner layers on both types of materials are not very different. It can be argued that the incorporation of Zn in a Cr_2O_3 type structure does not lead to such a large alteration of the properties of such phase when compared to the incorporation of Zn in FeCr_2O_4 type oxides.

The inner layer thicknesses for the oxides formed on Alloys 600 and 690 in both simulated and in-reactor PWR water in the absence or presence of Zn in the water are compiled in Figure 43 as depending on exposure time. In the figure, the experimentally determined thickness values are compared with the thickness calculated according to equation (14). Once again a reasonable agreement is obtained without any further adjustment of parameters, which demonstrates the

ability of the model to predict the kinetics of growth of the oxide on nickel-based alloys as well.

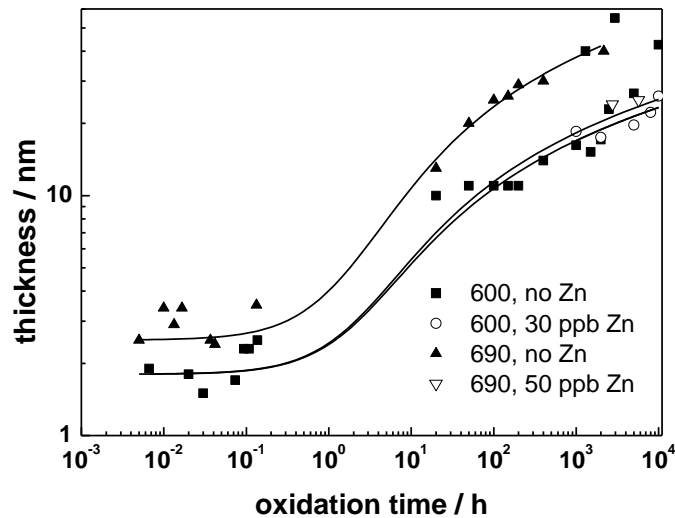


Figure 43 Inner layer thickness vs. time data for nickel-based alloys in simulated and in-reactor PWR water with or without Zn addition at 260-325°C (symbols) and calculated curves according to the model (solid lines).

9.4 System response to zinc transients

Analysis of plant responses to transients in power production and zinc injection rates has the potential to reveal additional information about how, where, and at what rate zinc is deposited and incorporated into the films on primary system surfaces. Although the process of zinc transport and incorporation is complicated by the numerous mechanisms and surfaces available for incorporation, a control theory type analysis (linear system analysis) could be useful for analysis of transients, including initial injection of zinc, normal plant transients (such as shifts in core boiling or coastdown at end of cycle), and off-normal plant transients (such as responses to unplanned shutdowns) [78].

Figure 44 shows a simple example block diagram for a prototypical four loop plant [78]. In this example, zinc is injected and measured in the CVCS. The complicated processes of zinc deposition in the core and in each of the ex-core steam generator surfaces are represented by one simple block each. The relationship between the zinc injection rate and the measured zinc concentration can be modelled using differential equations. The remaining unknowns are considered to be the magnitudes of the source and sink terms. These terms may be obtained by evaluating the differences between responses to specific zinc injections under different plant conditions.

Taking the action of zinc on fuel as an example, the authors [78] assumed that zinc may be incorporated into the crud in the following two manners:

- Initial surface incorporation, which is reversible and has a rate that is dependent on the difference between the local RCS zinc concentration and the theoretical saturation concentration associated with the crud. It is further assumed that this incorporation takes place through two parallel processes, boiling and non-boiling.

- Subsequent incorporation into the bulk deposit, which is permanent and has a rate that is dependent on the mass on the deposit surface.

A schematic of these processes and their interaction with the three relevant zinc masses is shown in Figure 45.

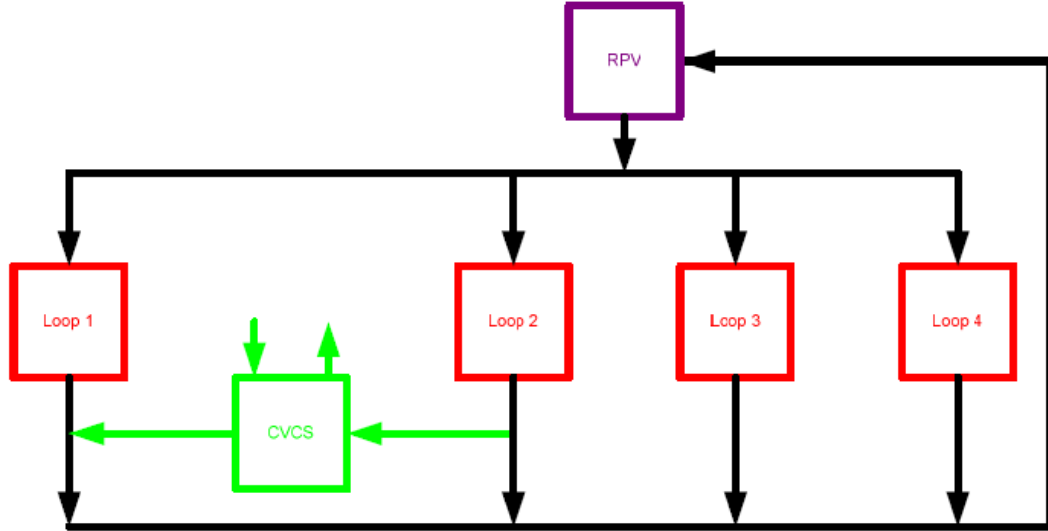


Figure 44 Block Diagram for a Prototypical Four Loop Plant [78].

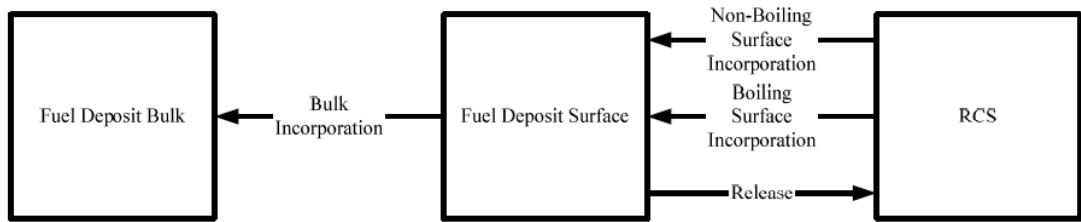


Figure 45 Schematic Fuel Deposit Zinc Model [78].

According to Marks et al. [78], the following differential equation summarizes the model element discussed above

$$\frac{dm_{\text{fuel deposit surface}}}{dt} = r_{\text{non-boiling}} + r_{\text{boiling}} - r_{\text{release}} - r_{\text{incorporation,bulk}} \quad (15)$$

where

$$r_{\text{non-boiling}} = h_{\text{non-boiling}} \Delta c_{lm,core} A_{\text{fuel}} \rho_{\text{water}}, r_{\text{boiling}} = \frac{dM}{dt} \frac{c_{RCS,core \text{ inlet}} + c_{RCS,core \text{ outlet}}}{2}$$

$$r_{\text{release}} = k_{\text{release}} \Delta c_{lm,core} A_{\text{fuel}} \rho_{\text{water}}, r_{\text{incorporation,bulk}} = k_{\text{incorporation,bulk}} m_{\text{fuel deposit surface}}$$

$h_{\text{non-boiling}}$ - mass transfer coefficient to crud surface (derived from empirical correlations)

$\Delta c_{lm,core}$ - log mean difference of concentrations, A_{fuel} - fuel area, ρ_{water} - water density, (16)

k_{release} - release rate constant (chemically activated process)

$\frac{dM}{dt}$ - boiling rate of the entire core, $k_{\text{incorporation,bulk}}$ - incorporation rate constant

To estimate the equilibrium concentration of Zn at the surface of the crud, adsorption equilibrium of the type described by equation (13) was used, and after suitable transformations the authors arrive at an expression of the type (for example, at the inlet)

$$C_{crud,core\ inlet} = \frac{\left(\frac{m_{Zn,crud}}{m_{Zn,total}}\right)^2 H_2O [H^+]}{\left\{1 - 2\left(\frac{m_{Zn,crud}}{m_{Zn,total}}\right)\right\}^2 K_{ads,inlet}} AW_{Zn} \quad (17)$$

where $K_{ads,inlet}$ is the equilibrium constant for adsorption at the inlet and AW_{Zn} the atomic weight of zinc. An example for a calculation based on equation (17) for several temperatures and surface coverages is shown in Figure 46. In this figure, calculated values are shown for the following representative temperatures:

- 300°C is used as a typical hot standby temperature (i.e., essentially zero power production, but no cooldown)
- 315°C is used as an average steam generator temperature (i.e., midway between hot leg and cold leg temperatures)
- 335°C is used as the average fuel surface temperature (i.e., midway between hot leg and pressurizer temperatures – the approximate temperature at which sub-cooled nucleate boiling occurs on the fuel surface)

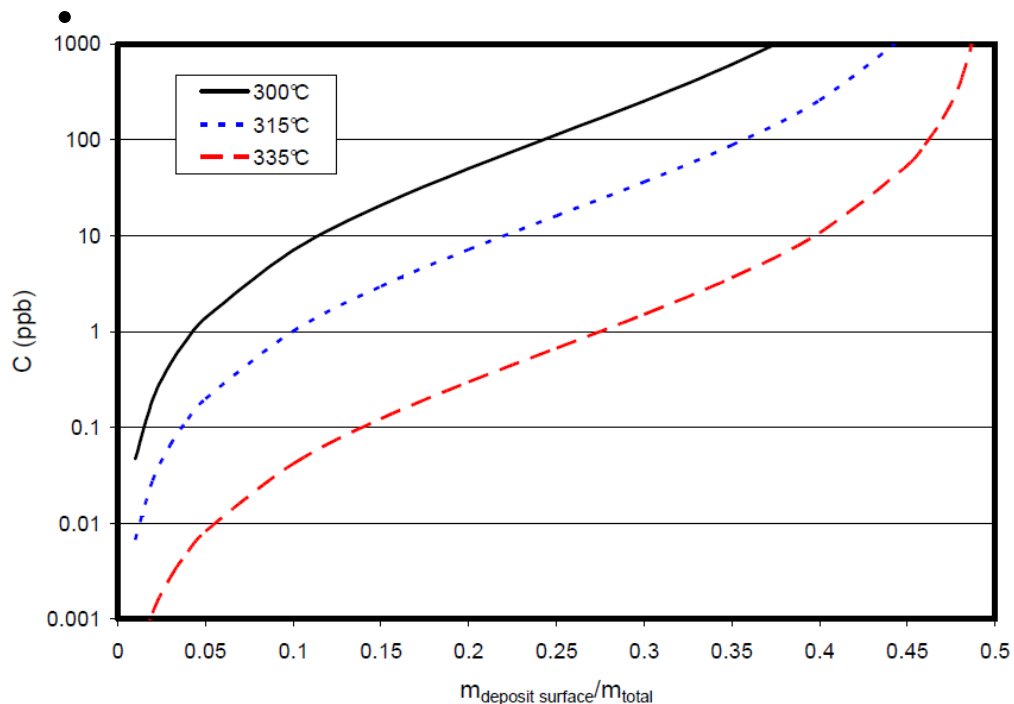


Figure 46 Equilibrium Bulk Concentrations as a Function of the Fraction of Adsorption Sites Filled using MULTEQ calculated zinc solubilities.

The model elements derived in Ref. 78 combine to form a highly complex description of the behavior of zinc in the primary system. Unfortunately, the complexity of the model makes it impractical for several reasons, including the following:

- The model introduces too many unknown parameters. For appropriate benchmarking evaluations of these parameters numerous sets of plant data would need to be analyzed.
- Even if an extensive benchmarking were to be performed, the large number of unknown parameters would make separation of plant specific, cycle-specific, and event-specific phenomena very difficult.
- The estimation of several parameters requires data that is not generally available.

Therefore, the model elements were evaluated to develop insights into the behavior of zinc without actually solving the model. The following conclusions have been reached from such a preliminary treatment:

- One important conclusion from the development of the model is that the steam generator tubes and the fuel cladding are the most important surfaces with respect to zinc. However, less zinc is transferred to the letdown heat exchangers than would be predicted based solely on available area because the mass transfer coefficients for the letdown heat exchangers is substantially less than for the steam generators or the fuel due to the lower temperature (this is mostly a viscosity effect).
- The increase in zinc concentration in the boiling area, although not enough to precipitate zinc on the fuel surface, does lead to an increase in the extent of adsorption site saturation. However, as shown in Figure 46, at typical fuel surface temperatures ($\sim 340^{\circ}\text{C}$) increases in concentration (above, for example, approximately 10 ppb) result in only small increases in the surface saturation. Therefore, changes in the extent and location of boiling during a cycle are not expected to lead to significant zinc transients.
- The zinc concentration increase experienced during a power decrease (a reduction to zero power hot standby in the example above) is due to desorption from RCS surfaces and that the zinc entering the coolant comes in roughly equal portions from the fuel and the steam generators, with a higher release per area from the fuel compensated by the lower surface area, relative to the steam generators.

10 Conclusions and Outlook

Zinc injection into the reactor coolant system has been successfully performed at approximately 70 pressurized water reactors worldwide since the mid-1990s. The application of zinc injection has led to a reduction in standard radiation monitoring programme dose rates throughout the fleet, although some data suggest that its addition can elevate the concentrations of other radioisotopes such as ^{58}Co in the coolant.

The primary driving force for injecting zinc is the opportunity to obtain dose rate reductions. In other cases, zinc injection is part of a plant's overall materials reliability programme aimed at mitigating primary water stress corrosion cracking initiation. The Electric Power Research Institute (EPRI) has ongoing research in radiation field management, materials and fuel reliability related to zinc injection. These programmes align with ongoing efforts to increase fuel performance and equipment reliability as well as balancing the radiation field management

challenges. This summary is an up-to-date review of the current industry status related to zinc injection.

The number of PWRs injecting zinc into the primary system has increased from 17 units in 2004 to 73 in 2010, with 10 more planned within the next two years. This represents about 27% of the operating PWRs in the world and 56% of the PWRs in the U.S. By the end of 2011 the percentage of PWRs injecting zinc is expected to increase to approximately 31% worldwide. Plants inject zinc for two primary reasons: dose rate reduction and PWSCC initiation mitigation. Additional goals for zinc injection programmes are to mitigate corrosion product generation and crud deposition on fuel surfaces. Approximately 85% of the plants injecting zinc report dose rate reduction as the primary goal, with the remainder identifying PWSCC mitigation and crud mitigation as the primary drivers. Typical zinc injection strategies employ RCS zinc concentrations of 5-20 ppb. Additional plant experience with zinc concentrations as high as 35-40 ppb has also been obtained.

Zinc injection achieves the noted benefits via mechanisms at the molecular level. As zinc is incorporated into the oxide films of wetted surfaces in an operating PWR, it changes the morphology and composition of oxide films, thereby changing their corrosion characteristics. In addition, it is believed that zinc displaces iron, nickel and cobalt from the crystalline lattice sites in the inner oxide layer on the materials of system surfaces. With exposure time, this process makes the oxide layers thinner, more stable and more protective.

10.1 Zinc impact on PWR primary chemistry

Farley Unit 2 was the first plant to inject zinc starting in 1994. Farley used naturally-occurring zinc acetate and targeted an RCS zinc concentration of 35-40 ppb. In the presence of a neutron flux, ^{64}Zn can absorb a neutron to become ^{65}Zn , which is radioactive (1.1 MeV gamma) with a 243.8 day half-life. Therefore, plants adding natural zinc experience a smaller radiation dose benefit because of the production of ^{65}Zn . Similarly high target zinc concentration programmes were implemented in the U.S. at Farley 1, Diablo Canyon 1 and 2 and Beaver Valley 1. In the mid-1990s, the large difference in cost between natural and depleted zinc favoured injection programmes using natural zinc.

Subsequent zinc injection projects using depleted zinc demonstrated that additional dose rate reductions could be achieved. Depleted zinc does not introduce ^{64}Zn into the coolant, thereby avoiding the creation of ^{65}Zn and enabling greater dose rate reductions. To date all of the plants that once employed natural zinc have transitioned to depleted zinc, a shift further supported by the significant cost reduction in depleted zinc. Additionally, all of these plants noted a reduction, or levelling, in system zinc demand and an increase in the contribution of ^{65}Zn to the dose-impacting radioisotopes while still using natural zinc.

A significant amount of RCS chemistry data has been collected as part of the utility-specific zinc programmes over the past several years. The EPRI PWR Zinc Users Group sponsored research to assess the impact of RCS zinc addition on nickel and radiocobalt concentrations during both operating and shutdown periods to determine if plant responses to initial zinc injection could be predicted.

10.1.1 Nickel

A principal concern regarding the plant response to initial injection is that dissolved zinc will interact with ex-core oxide films in a manner that releases nickel into the primary coolant system. Nickel released by this mechanism could deposit in the core and challenge fuel performance. Primary system chemistry data (principally nickel concentrations and radiocobalt activities) were evaluated for the cycles in which zinc was first injected. Assessments included comparisons of concentrations and activities before and after zinc injection as well as comparison of these periods to similar times in previous cycles. The mass of nickel released during shutdown was also assessed. The assessments did not discern a statistically significant increase in coolant nickel concentration upon initial zinc injection. However, the statistical evaluations of data from several units evaluated were inconclusive in this regard; that is, there could have been a nickel response at some low level but it could not be validated with the statistical tests used. There was no statistically significant increase in the mass of nickel released during shutdown chemistry manoeuvres following the initial zinc injection.

10.1.2 Radiocobalts

The impact of the first injection of zinc on primary coolant radiocobalt activities was assessed using raw data from several units and using published data from several others. The results indicate that radiocobalt responses have been observed at some units, but not others. The analysis could not identify a factor that could be correlated to whether or not a unit showed a radiocobalt response. Regular updates to these evaluations to assess the longer-term impacts of zinc injection on RCS nickel and radiocobalt concentrations are planned. These results, while limited to the impacts identified during the initial zinc injection cycle, indicate that further assessment is warranted of the mechanism by which zinc is incorporated into the RCS oxide layers. Additionally, these data suggest that while an increase in radiocobalt levels may not occur in conjunction with zinc injection, one should be prepared for such.

10.2 Zinc impact on fuel

An extensive programme is running in a range of countries to ensure that fuel integrity and performance are not challenged by zinc injection. Based on fuel surveillance programmes at six plants with increasing fuel duty, several observations have been made to date:

- Zinc has not caused an increase in fuel cladding corrosion at any of the reported campaigns
- No abnormal buildup of crud has been observed
- No fuel performance issues (such as AOA/CIPS) have been reported that were directly related to zinc.

The experience base for high-duty plants injecting zinc continues to grow. There are currently eight high-duty plants injecting zinc that have done so successfully, obtaining dose rate reduction and materials benefits, with no reported fuel concerns. For high-duty plants, a risk assessment specific to the cycle and zinc injection

strategy is an important part of the overall zinc injection program. Byron 1 and Braidwood 1, the two highest-duty four-loop PWRs in the U.S., successfully implemented zinc addition in 2010. The first cycle of injection at Braidwood 1 concluded in the autumn of 2010 with no reported negative fuel impacts. The first cycle of injection at Byron 1 will conclude in the spring of 2011.

Plants injecting zinc have used a combination of fuel cladding, including Zircaloy-4, ZIRLO, low-tin Zircaloy, M5, OPTIN and various combinations of these claddings. Industry exposure for the three highest exposure claddings demonstrated no effect of zinc on oxide growth, with ZIRLO cladding having the highest exposure.

10.3 Zinc impact on PWR dose rates

As part of the standard radiation monitoring and chemistry monitoring and assessment programmes, refuelling outage dose rate data, and start-up, shutdown and operating plant chemistry data is collected for plants worldwide. Trending of refuelling outage dose rate data and shutdown chemistry releases continues to show trends of reduced dose rates and releases for plants injecting zinc. Initially developed correlations between zinc exposure and dose rate reductions as measured at standardized survey points for plants with Alloy 600, Alloy 690 and Alloy 800 steam generator tubing material have been subsequently verified and updated. A comprehensive dataset of cumulative dose reductions to zinc exposure for the different steam generator (SG) tubing materials has been created and logarithmically fitted. These correlations have been used to predict potential dose rate reductions resulting from specific zinc programmes and to assess the efficacy of a completed zinc injection cycle. In general, the reduction in both hot leg and cold leg dose rates were achieved as a result of zinc injection at plants with Alloy 690TT, and Alloy 600MA and 600TT steam generator tubing.

It should be noted that initially Alloy 600 and 690 have been found to behave slightly differently and the behaviour pertinent to those materials do not take into account SG tubing manufacturing processes or release rates observed in these different materials. These dose rate reduction correlations are in the process of being revised to support the in-process revision of the PWR zinc application guidelines. In summary, reductions in shutdown dose rates have been routinely observed at PWRs following zinc addition.

10.4 Outlook

Primary coolant chemistry is the result of different compromises for getting benefits and/or limiting the risks on several domains: fuel performance, field radiation, material integrity and environmental impacts. NPP operational experience and laboratory results show that zinc injection application provides positive effects in all of these domains apparently without inducing adverse impacts.

Zinc water chemistry continues to be one of the consistent options for dose rate reduction. A complete understanding of plant materials, core design and chemistry issues is essential prior to commencing a zinc injection programme. Consistent with

EPRI Pressurized Water Reactor Primary Water Chemistry Guidelines, as well as newly developed regulatory documents in Europe and Japan, a nuclear utility's primary chemistry strategic plan should, as a minimum, review and document the bases for injecting zinc or not.

Even if the popularity of zinc injection is due to its fast impact on surface contamination, the main interest of zinc injection is its multiple benefits not only for dose rates reduction but also for PWSCC and AOA mitigation. The zinc injection should be considered as a strategy with benefits in short, medium and long term. Its application as soon as possible in the life of NPPs, perhaps already at the HFT stage, and especially before steam generator replacement and fuel cycles modifications seems to be an important decision that would contribute to ensure the passivation process of new components, fuel performance, the full power operation of the units and most probably an extension of the service life of materials and components.

Further works on thermodynamics and kinetics of zinc incorporation processes, its effect on oxide thermodynamic properties, composition, structure and morphology, as well as more detailed "zinc crud" characterisation will help to achieve a new level of understanding of zinc behaviour in primary coolant in order to optimise the practice for any kind of unit: high, low duty, with or without load following, as well as with high or low dose rates.

11 Summary

This report describes the use of zinc injection technology in Pressurized Water Reactor (PWR) plants worldwide. The review covers the range from basic information to current knowledge and understanding of operational behaviour. The basis of this report is the information available in the open literature, including proceedings of the recent International Conferences on Water Chemistry of Nuclear Reactor Systems. The influence of zinc injection in the primary circuit of PWRs on corrosion release, oxide growth on construction materials (stainless steels and nickel-based alloys), activity incorporation and source term reduction, fuel cladding corrosion, build-up and transformation of fuel crud, and Primary Water Stress Corrosion Cracking is described from the viewpoint of both laboratory testing and plant operational experience in France, USA, Germany and Japan. The perspectives to employ zinc water chemistry already at the stage of Hot Functional Testing, as well as for the use of zinc injection in WWERs are also presented and discussed. A substantial part of the present report is devoted to the recent experience in the modelling of the influence of zinc on corrosion and activity build-up in PWRs. Thermodynamic calculations of stability of different oxide phases and their solubility are critically reviewed. Solid-state chemical calculations of the defect structure of oxides on construction materials are also briefly reviewed. The kinetic modelling of the zinc adsorption on and incorporation into oxides on stainless steels and nickel-based alloys in simulated and in-pile PWR conditions is presented in detail and the significance of the derived kinetic parameters for the evaluation of the role of zinc in corrosion mitigation and activity build-up suppression is discussed. Finally, a formal linear system approach to the effect of zinc transients in PWRs is briefly outlined and an outlook of the current state-of-the art of our knowledge of zinc water chemistry and its future perspectives is given.

References

1. J.N. Esposito, G. Economy, W.A. Byers, J.B. Esposito, F.W. Pement, R.J. Jacko, C.A. Bergmann, The Addition of Zn to the Primary Reactor Coolant for Enhanced PWSCC Resistance, in Proc. 5th International Symposium on Environmental Degradation of Materials in Nuclear Power Systems - Water Reactors, American Nuclear Society, La Grange Park, USA, 1991, p. 495.
2. B. Stellwag, U. Staudt, Dosisleistungsreduktion in Kernkraftwerken durch Zinkdosierung – Grundprozesse und Schlussfolgerungen für den Anlagenbetrieb, VGB- Konferenz, VGB-TB 431(1995).
3. K. Fruzzetti, S. Choi, C. Haas, M. Pender, D. Perkins, in Proc. Intern. Conference on Water Chemistry in Nuclear Power Plants, Quebec, Canada, 2010, paper 6.01.
4. Winkler, R. and Lehmann, H. Zur Qualitätsbewertung oxidischer Korrosionsschutzschichten, VGB Kraftwerkstechnik, 1985, 65, 421-426.
5. D. H. Lister, R. D. Davidson, E. McAlpine, The mechanism and kinetics of corrosion product release from stainless steel in lithiated high temperature water, Corros. Sci. 27(1987)113-127.
6. B. Beverskog, The role of Zn in LWRs, in Proceedings of the International Conference on Water Chemistry of Nuclear Reactor Systems, San Francisco, Oct. 11-14, 2004, paper 2.7, p.117-130.
7. Ahlberg E., Rebensdorff B., General Corrosion of Alloy X-750 under BWR Conditions, In Proc. BNES Conf. water Chemistry Nucl. Reactor Syst. 6, Bournemouth, UK, 12-15 Oct. 1992, Vol. 2, 278-5/8, 1992.
8. A. Tigras, B. Stellwag, N. Engler, J.L. Bretelle, A. Rocher, Understanding the zinc behavior in PWR primary coolant: a comparison between French and German experience, in Proceedings of NPC'08, Berlin, Germany, September 7-13, 2008, paper 1.01.
9. A. Tigras, G. Debec, B. Jeannin, A. Rocher, EdF Zinc Injection: Analysis of Power Reduction Impact on the Chemistry and Radiochemistry parameters, Proceedings of the International Conference on Water Chemistry in Nuclear Power Plants, Jeju, Korea, 2006, paper 2.1.
10. D. Perkins, K. Ahluwalia, J. Deshon, C. Haas, An EPRI perspective and overview of PWR Zinc injection, in: Proceedings of International Conference on Water Chemistry of Nuclear Reactor Systems, VGB, Berlin, 2008, paper P2-26.
11. S.E. Ziemniak, M. Hanson, Corrosion behavior of 304 stainless steel in high temperature, hydrogenated water, Corros. Sci. 44 (2002) 2209–2230.
12. S.E. Ziemniak, M. Hanson, P.C. Sander, Electropolishing effects on corrosion behavior of 304 stainless steel in high temperature, hydrogenated water, Corros. Sci. 50 (2008) 2465–2477.
13. S.E. Ziemniak, M. Hanson, Zinc treatment effects on corrosion behavior of 304 stainless steel in high temperature, hydrogenated water, Corros. Sci. 48 (2006) 2525–2546.
14. J. Korb, B. Stellwag, Thermodynamics of zinc chemistry in PWRs: effects and alternatives to zinc, Nuclear Energy 36 (1997) 377–383.
15. K. Miyajima, H. Hirano, Thermodynamic consideration on the effect of Zinc Injection into PWR primary coolant for the reduction of radiation buildup and corrosion control, in: CORROSION-2001, NACE, Houston, 2001, Paper No. 01143.

16. Xiahe Liu, Xinqiang Wu, En-Hou Han, Influence of Zn injection on characteristics of oxide film on 304 stainless steel in borated and lithiated high temperature water, *Corros. Sci.* (2011), <http://dx.doi.org/10.1016/j.corosci.2011.06.011>
17. I. Betova, M. Bojinov, P. Kinnunen, K. Lundgren, T. Saario, Influence of Zn on the oxide layer on AISI 316L(NG) stainless steel in simulated pressurised water reactor coolant, *Electrochim. Acta* 54 (2009) 1056-1069.
18. S.E. Ziemniak, M. Hanson, Corrosion behavior of NiCrFe Alloy 600 in high temperature, hydrogenated water, *Corros. Sci.* 48 (2006) 498–521.
19. S.E. Ziemniak, M. Hanson, Zinc treatment effects on corrosion behavior of Alloy 600 in high temperature, hydrogenated water, *Corros. Sci.* 48 (2006) 3330-3348.
20. H. Kawamura, H. Hirano, S. Shirai, H. Takamatsu, T. Matsunaga, K. Yamaoka, K. Oshinden, H. Takiguchi, Inhibitory Effect of Zinc Addition to High-Temperature Hydrogenated Water on Mill-Annealed and Prefilmed Alloy 600, *Corrosion* 56 (2000) 623–637.
21. Junbo Huang, Xiahe Liu, En-Hou Han, Xinqiang Wu, Influence of Zn on oxide films on Alloy 690 in borated and lithiated high temperature water, *Corros. Sci.* 53 (2011) 3254-3261.
22. Liu Xia-he, Wu Xin-qiang, Han En-Hou, Status and Progress on Study of Corrosion Behavior of Structural Materials in Zn-injected Waters for LWRs, *Corros. Sci. Protect. Technol.* 23(2011)287-292.
23. A. Tigras, A. Stutzmann, O. Bremnes, M. Claeys, G. Ranchoux, J.C. Segura, J. Errera, S. Bonne, Zinc injection implementation process at EdF: risk analysis, chemical specifications and operating procedures, in *Proceedings of NPC 2010, Quebec, October 3-7, 2010*, paper 1.02.
24. A. Tigras, F. Dacquait, L. Viricel, J.C. Segura, L. Guinard, J.-L. Bretelle, A. Rocher, Complete Analysis of Zinc Injection Impact at Bugey 2 & 4, in *Proceedings of NPC'08, Berlin, Germany, September 7-13, 2008*, paper P1.32.
25. EPRI Pressurized Water Reactor Zinc Application Guidelines, EPRI, Palo Alto, CA; 2006, 1013420.
26. A. Proust, M. Guillodo, M. Barale, S. Perrin, M. Pijolat, K. Wolski, P. Combrade, Determination of the kinetics of oxidation and cation release of Ni base alloys in PWR primary coolant, in *Proceedings of NPC'08, Berlin, Germany, September 7-13, 2008*, paper L03-2.
27. F. Roumiguère, Field Experience on Zn Injection on PWR Plants With a View to Dose Rate Reduction, in *Proc. International Conference Nuclear Energy for New Europe 2005, Bled, Slovenia, September 5-8, 2005*, paper 0103.
28. B. Stellwag, J. Haag, B. Markgraf, D. Preiksich, D. Wolter, Short-Term and Long-Term Effects of Zinc Injection on RCS Chemistry and Dose Rates at Siemens PWR Plants, *Proc. Int. Conference Water Chemistry of Nuclear Reactor Systems*, Oct. 11 – 14, 2004, San Francisco, EPRI, Vol. 1, Paper 2.6.
29. N. Nagata, H. Wada, E. Kadoi, K. Taniguchi, Y. Watanabe, H. Ikoma, T. Semba, T. Hamaguchi, Application of the Zinc Injection Technique for Reducing Radiation Source in PWR Nuclear Power Plants, *Jpn. J. Health Phys.*, 45 (2010) 57-64.
30. Ziemniak, S.E., Jones, M.E., Combs, K.E.S., Zinc(II) oxide solubility and phase behavior in aqueous sodium phosphate solutions at elevated temperatures (1992) *J. Solution Chem.* 21 (11), pp. 1153-1176.

31. Bénézeth, P., Palmer, D.A., Wesolowski, D.J. The solubility of zinc oxide in 0.03 m NaTr as a function of temperature, with in situ pH measurement (1999) *Geochimica et Cosmochimica Acta*, 63 (10), pp. 1571-1586
32. Bénézeth, P., Palmer, D.A., Wesolowski, D.J., Xiao, C. New measurements of the solubility of zinc oxide from 150 to 350°C, *J. Solution Chem.* 31 (2002) 947-973.
33. Wesolowski, D. J., E. Ziemniak, L. M. Anovitz, M. L. Machesky, P. Bénézeth, D. A. Palmer, Solubility and surface adsorption characteristics of metal oxides". Chapter 14 in D.A. Palmer, R. Fernández-Prini and A.H. Harvey, Eds., *The Physical and Chemical Properties of Aqueous Systems at Elevated Temperatures and Pressures: Water, Steam and Hydrothermal Solutions*, Academic Press, pp. 493-595 (2004).
34. Byers, W.A., Wang G., J. Deshon, The limits of Zinc Addition in High Duty PWRs, Proc. International Conference on Water Chemistry of Nuclear Reactor Systems, Berlin, Germany, 2008, paper L13-4.
35. Materials Reliability Program: Technical Bases for the Chemical Mitigation of Primary Water Stress Corrosion Cracking in Pressurized Water Reactors (MRP-263). EPRI, Palo Alto, CA: 2009. 1019082.
36. Evaluation of Plant Data to Determine Effects of Zinc on Primary Water Stress Corrosion Cracking in Pressurized Water Reactors. EPRI, Palo Alto, CA: 2005. 1011775.
37. Evaluation of Plant Data to Determine Effects of Zinc on PWSCC: 2008 Revision. EPRI, Palo Alto, CA: 2008. 1016558.
38. Materials Reliability Program: Mitigation of Stress Corrosion Crack Growth in Nickel-Based Alloys in Primary Water by Hydrogen Optimization and Zinc Addition (MRP-280). EPRI, Palo Alto, CA: 2010. 1021013.
39. T.M. Angeliu, P.L. Andresen, Effect of zinc additions on oxide rupture strain and repassivation kinetics of iron-based alloys in 288 °C water, *Corrosion* 52 (1996) 28-35.
40. D.S. Morton, D. Gladding, M.K. Schurman, C.D. Thompson, Effect of Soluble Zinc Additions On the SCC Performance of Nickel alloys in deaerated hydrogenated water, Proc. of the Eighth International Symposium on Environmental Degradation of Materials in Nuclear Power Systems-Water Reactors, Amelia Beach, FL, NACE, August 1997, 387-395.
41. H. Kawamura, H. Hirano, S. Shirai, H. Takamatsu, T. Matsunaga, K. Yamaoka, K. Oshinden, H. Takiguchi, The Effect of Zinc Addition to Simulated PWR Primary Water on the PWSCC Resistance, Crack Growth Rate and Surface Oxide Film Characteristics of Prefilmed Alloy 600, *CORROSION'98*, NACE, Houston, TX, 1998, paper No.141.
42. P.L. Andresen, J.A. Wilson, K.S. Ahluwalia, Use of Primary Water Chemistry in PWRs to mitigate PWSCC of Ni-base alloys, Proceedings of the International Conference on Water Chemistry in Nuclear Power Plants, Jeju, Korea, 2006, paper 2-5.
43. W.Y. Maeng, Y.S. Chu, U.C. Kim, Effect of Zinc Injection on the SCC Crack Growth of Alloy 600 in Water at 360°C, Proceedings of the International Conference on Water Chemistry in Nuclear Power Plants, Jeju, Korea, 2006, paper 2-4.
44. P. Andresen, Effect of Primary Water Zinc Injection on PWSCC in Ni-Based RCS Components, MRP/PWROG Mitigation Briefing to NRC RES, 2007.

45. C. Marks, PWSCC Chemical Mitigation: Hydrogen Optimization and Zinc Injection, Industry Briefing to the NRC on PWSCC Mitigation Research, Rockville, MD, 2008.
46. Nobuaki Nagata, Hideaki Ichige, Eiichi Kadoi, Yoshifumi Watanabe, Hideya Ikoma, Tsuyoshi Semba, Toshiaki Hamaguchi, Progress of the Zinc Injection in Tsuruga NPP Unit 2, 2006 ISOE Asian ALARA Symposium, October 2006.
47. H.-U.Sell, U. Straudt, B. Stellwag, PWR Fuel Performance and Zinc Injection, Proceedings of the International Conference on Water Chemistry in Nuclear Power Plants, Jeju, Korea, 2006, paper 7.4.
48. Jayashri N. Iyer, E. F. Pulver, D. Mitchell, J. McInvale, K. G. Turnage, J. Deshon, ZIRLO™ Clad Fuel Performance in Zinc Environments at High Duty Plants-an Update, Proceedings of the International Conference on Water Chemistry in Nuclear Power Plants, Jeju, Korea, 2006, paper 7.5.
49. P.Guillermier, J. Thomazet, H.-J. Sell, L. Lamana, R. Montgomery, C.Faulkner, J.Lemons, Proc. International Conference on Water Chemistry of Nuclear Reactor Systems, Berlin, Germany, 2008, paper L13-2.
50. J. N. Iyer, K. Kargol, J. Gardener, K. Bieze, ZIRLO™ Clad Fuel Performance in Simultaneous Zinc and Elevated Lithium Environments, Proc. International Conference on Water Chemistry of Nuclear Reactor Systems, Berlin, Germany, 2008, paper L13-3.
51. Axial Offset Anomaly (AOA) Mechanism -Verification in Simulated PWR Environments, EPRI ENUSA_Studsvik CA, 1013423, 2006.
52. W. A. Byers, J. Deshon, G. P. Gary, J. F. Small, J. B. Mcinvale, Crud Metamorphosis at the Callaway Plant, Proceedings of the International Conference on Water Chemistry in Nuclear Power Plants, Jeju, Korea, 2006, paper 7.3.
53. P. Srisukvatananan, D.H. Lister, Nickel Ferrite Deposition onto Heated Zircaloy-4 Surfaces in High-Temperature Water with Subcooled Boiling; Preliminary Study of the Effects of pH and Zinc Addition, Proceedings of the International Conference on Water Chemistry in Nuclear Power Plants, Jeju, Korea, 2006, paper 7.6.
54. W. A. Byers, G. Wang, J. C. Deshon, The Limits of Zinc Addition in High Duty PWRs, Proc. International Conference on Water Chemistry of Nuclear Reactor Systems, Berlin, Germany, 2008, paper L13-4.
55. Jei-Won Yeon, In-Kyu Choi, Kyoung-Kyun Park, Hyoung-Mun Kwon, Kyuseok Song, Chemical analysis of fuel crud obtained from Korean nuclear power plants, J. Nucl.Mater. 404 (2010)160-164.
56. Fuel Reliability Guidelines: PWR Fuel Cladding Corrosion and Crud. EPRI 1015499, Palo Alto, CA 2008.
57. Solubility of Zinc Silicate and Zinc Ferrite in Aqueous Solution at Light Water Reactor Temperatures. EPRI 1015035, Palo Alto, CA: 2007.
58. D.A. Palmer, L. M. Anovitz, L. L. Wilson, Solubility of Zinc Silicate and Zinc Ferrite in Aqueous Solution to High Temperatures, Proc. 15th International Conference on the Properties of Water and Steam, Berlin, September 8–11, 2008, paper 5-04.
59. H.Hayakawa, Y. Mino, S. Nakahama, Y.Aizawa, T. Nishimura, R. Umehara, Y. Shimuz, N. Kogawa, Z. Ojima, in Proceedings of NPC 2010, Quebec, October 3-7, 2010, paper 1.15P.
60. V.A. Yurmanov, V. N.Belous, E.V. Yurmanov, S.V. Filimonov, D.V. Timofeyev, Prospects for zinc injection in Russian design reactors, in Proceedings of NPC 2010, Quebec, October 3-7, 2010, paper 1.19P.

61. Alexeev, B.A., Ermakov, V.A., Chernorotov, E.S. et al. Water chemistries and corrosion of materials in water cooled and moderated power reactors. 2nd Symposium "Water chemistry of nuclear reactors and radiation monitoring". Eastern Germany. 1972.
62. Martynova, O.I., Nazarov, A.I. et al. Primary coolant activity of boiling reactor VK-50 type. Atomic energy. V.23. No.4. October 1967.
63. Yakshin, E.K., Chechetkin, Y.V. et al. Fission product calculation technique in primary system of boiling reactor. Atomic stations. Issue 5. Moscow. Atomizdat. 1983. p.177-182.
64. Yurmanov, V.A., Turbaevsky, V.V., Filimonov, S.V., Skorynin, G.M., Timofeev, D.V. et al. Technical and economic evaluation of radiation exposure reduction based on zinc injection. The 7th International conference on Safety, Efficiency and Economics of Nuclear Power Industry, Concern Rosenergoatom, Moscow, 26-27 May 2010. Abstracts of papers. P.105-107.
65. V. Švarc, K. Šplíchal, J. Kysela, K. Andrová, V. Hanus, I. Petrecký, P. Marcinský, I. Smieško, Primary Water Chemistry of WWER Reactors: Comparison of Loop Experiments with Hydrogen, Ammonia and Zinc, Proceedings of the International Conference on Water Chemistry in Nuclear Power Plants, Jeju, Korea, 2006, paper P1.6.
66. Yurmanov, V.A., Povalishin, N.B., Arkhipenko, A. Development of WWER primary water chemistry guidelines. International conference on water chemistry of nuclear reactor systems. 15–18.09.2008, Berlin, Germany. Paper L02-2.
67. K. Makela, T. Laitinen, M. Bojinov, The influence of modified water chemistries on metal oxide films, activity build-up and stress corrosion cracking of structural materials in nuclear power plants, STUK-YTO-TR 152. Helsinki 1999. 55 pp.
68. A. Navrotsky O. J. Kleppa, The thermodynamics of cation distributions in simple spinels, J. Inorg. Nucl. Chem. 29(1967)2701-2714.
69. D.H. Lister, Activity Transport and Corrosion Processes in PWRs, Nuclear Energy 32 (1993) 103–114.
70. Betova, I.; Bojinov, M.; Kinnunen, P.; Lundgren, K.; Saario, T. A Mixed-Conduction Model for the Oxidation of Stainless Steel in a High-temperature Electrolyte. Estimation of kinetic parameters of individual inner layer constituents J. Electrochem. Soc. 2008, 155, C81-C92.
71. Betova, I.; Bojinov, M.; Kinnunen, P.; Lundgren, K.; Saario, T. A kinetic model of the oxide growth and restructuring on structural materials in nuclear power plants. Chapter 3 in Structural Materials and Engineering, F. Nagy, Ed., Nova Publishers, 2009, 91-133.
72. Betova, I., Bojinov, M., Kinnunen, P., Lehikoinen, J., Lundgren, K., Saario, T. An integrated deterministic model for activity build-up and corrosion phenomena in LWRs. Proceedings of ICAPP'07, SFEN, Avignon, France, 2008, paper No. 7122.
73. Lister, D.H.; Venkateswaran, G. Effects of magnesium and zinc additives on corrosion and cobalt contamination of stainless steels in simulated BWR coolant, Nucl. Technol. 1999, 125, 316-331.
74. Bojinov, M.; Kinnunen, P.; Olin, M. ANTIOXI -Incorporation of coolant originating cations into the oxide films on stainless steels - experiments and modelling, VTT-R-10851-07, VTT Technical Research Centre of Finland, Espoo, 2008.
75. Barale, M., Mansour, C., Carrette, F., Pavageau, E.M., Catalette, H., Lefèvre, G., Fedoroff, M., Cote, G., Characterization of the surface charge

- of oxide particles of PWR primary water circuits from 5 to 320 °C, J. Nucl. Mater. 2008, 381, 302-308.
76. Bennett, P.J.; Gunnerud, P.; Loner, J.; Petersen, J.K.; Harper, A. The effects of zinc addition on cobalt deposition in PWRs. *Water Chemistry of Nuclear Reactor Systems 7*, British Nuclear Energy Society, London, 1996; Vol.1, pp. 293-296.
77. Beverskog, B.; Mäkelä, K. Activity pickup in zinc doped PWR oxides. *Proc. of the JAIF International Conference on Water Chemistry in Nuclear Power Plants*, Japanese Nuclear Society, Kashiwazaki, Japan, 1998, p. 89-98.
78. C. Marks, R. Jones, D. Perkins, C. Haas, K. Fruzzetti, Analyses of System Responses to PWR Zinc Transients, International conference on water chemistry of nuclear reactor systems. 15–18.09.2008, Berlin, Germany. Paper P1-30.